# Simulation of a Wireless Communication Channel to Determine a Best Topology for a Base Station Array Antenna

Derek A. Wells

Thesis submitted to the Faculty of the
Virginia Polytechnic Institute and State University
in partial fulfillment of the requirements for the degree of

Master of Science
in
Electrical Engineering

Warren L. Stutzman, Chair
William A. Davis
Jeffrey H. Reed

January 24, 2003
Blacksburg, Virginia

Keywords: Array Antenna Topology, Beamforming, Channel Model, Diversity Combining, Simulation

# Simulation of a Wireless Communication Channel to Determine a Best Topology for a Base Station Array Antenna

Derek A. Wells

## (ABSTRACT)

This thesis presents simulation data on array operation in wideband communication systems. It is shown that array structures with closer inter-element spacing outperform structures with much larger inter-element spacing. It is also shown that circular structures outperform linear structures. This performance difference between the classifications of arrays is due largely to the circular array's ability to handle high levels of interference. Even though a diversity combining scheme (MRC) was used in the simulator, the arrays provided interference rejection capabilities due to the closely spaced antenna elements. Though diversity does provide a gain in received signal, relative to the faded signal, realized diversity gain only comes about once interference has been mitigated. This thesis work showed that in an environment with a lot of interferers, the rejection of those interferers by an array is of utmost importance, even more than fading mitigation.

The majority of this work was supported by LG Electronics of Seoul, Korea. A portion of the work was funded by the Defense Advanced Research Projects Agency (DARPA) and Raytheon of Arlington, VA and Lexington, MA, respectively. I am grateful for the sponsorship of academic research by these commercial and government entities.

# Acknowledgments

To Dr Warren L. Stutzman, Dr. William A. Davis and Dr. Jeff H. Reed, I say thank you. Many hours you have logged in pursuit of your education and your careers. In doing so, you have provided means for myself and many others to further our education, and our careers.

To the members of the Virginia Tech Antenna Group, I also say thank you. Many of you offered your technical expertise and insights when I asked. Specifically, I'd like to thank Kai Dietze and Gaurav Joshi for assistance on the topics of this thesis. Nathan Cummings and Ko-Ichiro Takamizawa deserve a round of applause for the computer hardware and software support they have provided. Byung-ki Kim, thank you for your technical insight you provided as well.

Seong-Youp Suh, you have been a good friend. Stanislav Licul, thank you for the many enjoyable discussions on world politics and finance and for loving America almost as much as I do. Laure Mousselon and Minh-Chau Huynh, thank you for your friendship. To R. Michael Barts, I want to say thanks for your friendship and for urging me to get involved in amateur radio. You have done more for my education than you'll ever know. Dr. Carl B. Dietrich, thank you for your insight of the thesis writing process and for being a friend.

# Contents

# List of Figures

# List of Tables

# Chapter 1

# Introduction

## 1.1 Motivation for Research

Approximately one year ago, the world celebrated the $100^{th}$ anniversary of Guglielmo Marconi's transatlantic radio transmission which occured on December 12, 1901. He had successfully transmitted and received signals over a few miles only a year or so earlier. Marconi had advanced the experiments of Heinrich Hertz to a level of patentable and commercially useful technology. This was the birth of radio. Today, many people rely heavily on radio in such fields as medicine, public safety, national defense, space exploration, scientific research, personal communications and entertainment. There have been many developments in radio technology for use in military and commercial applications. Many advancements in military applications for radio were developed prior to and during World War II (1939-1945). Since that time, a lot of research has been done in the areas of refining radio technology for advanced tasks. The area of personal comunications saw a dramatic shift to radio (wireless) in the 1990's. At that time, the end of the Cold War, many people with radio 'know-how' were developing what is now known as personal communications. Certainly similar technology had been seen in the United States for a decade or two, but in the 1990's, there was a significant number of years of economic prosperity, which developed a market for personal communications as we see it today. In the last half of the decade, the explosion of the Internet in day-to-day communications, business and entertainment has also changed the technology landscape. Now, there is a push for wireless internet, and wireless Local Area Network

(LAN). These trends were and are not exclusive to the United States. In fact, many countries around the world claim a larger 'wireless' population than the US. Regardless, wireless technology, which started 100 or more years ago, is close to being ubiquitous.

Military applications for wireless technology change as the military's needs change. Recently in the US military, there has been a major expansion in the use of unmanned surveillance vehicles (unmanned airborne vehicles, UAVs and unmanned ground vehicles, UGVs). Also, there is a desire to have a more field oriented (less centralized) military, in order to deploy smaller roving units with their own 'headquarters' in the field. Both of these concepts (unmanned vehicles and decentralized military) rely heavily upon wireless communication technology. Wireless military communications demand high levels of security, they employ electronic measures and countermeasures, they require reliability in adverse conditions, etc. These factors push the need for further research and development in wireless technology.

In terms of personal communications, the US, parts of Europe and Asia are currently at what is called $2^{nd}$ Generation (2G) wireless. 2G systems support voice and little else. $3^{rd}$ Generation, 3G, is the next step. In the development of $3^{rd}$ Generation (3G) Wireless Communication systems, steps are being taken to maximize capacity and increase quality of service over the current 2G systems. Bandwidths on the order of several Megahertz and data rates on the order of 2 Mbps for stationary users are expected to be the norm in 3G wireless systems. Voice transmission as well as data and video transmission are driving the need for increased bandwidth. The number of users in a given system is expected to increase. Interference will be a problem to contend with as the number of users per cell are increased. In order to save money in the personal communications industry and to increase capacity within current systems, work is being done to maximize the use of allotted spectrum and to optimize that portion of the communication infrastructure that is already in place. As long as the open commercial market continues to demand increases in system performance, research and development in personal communication system applications will continue.

For military and commercial wireless applications, research has been done via simulation methods and measurement campaigns. The purpose of such research is to investigate topics such as adaptive array algorithms, coding schemes (e.g. space-time coding), and spatial, angle and polarization diversity, to name a few. Many such studies are presented in the open literature. A topic that has been given very little treatment in the open literature in regards to modern wireless communication system performance is the topic of antenna

array geometry. It is understood that an array generally outperforms a single element. For this reason, arrays are desirable for deployment in modern communication systems. Due to constraints on size, arrays are not typically implemented at the mobile unit.[1] Realizing that a base station is generally not limited in size, power and processing capabilities, antenna arrays can be implemented at the base station sites in personal communication applications. As previously mentioned, certain military applications require roving headquarters. 'Base stations' are being created in military ground and airborne vehicles. Some of these mobile base stations require array antennas to provide proper coverage in communicating with other field units. With the aforementioned areas of ongoing research (algorithms, coding, diversity, etc.), the question arises, "Can a system's performance improve with the use of a certain array geometry?".

Certainly, there are some particularly bad choices for array topology in terms of spacing and element type that would severely degrade a system's performance, or render it useless. It is probable that a best array topology can be designed for a system that is highly constrained in its number and locations and types of users. But what about the general case? The general case is more realistic. In the general case, the number, locations and types of users is assumed to be within criterion margins, but these parameters are not tightly constrained. It is for the general case that simulations have been done and are reported here. The effects of base station array geometry on system performance is investigated. It is conceivable that arrays with particular types of geometries (i.e. linear, circular, etc.) might be shown to perform better than arrays of other geometry types. It also is possible, though unlikely, that a specific array geometry, rather than a class of geometries, can be determined to be the best possible configuration for the general wireless communications system. This study, through simulation data, poses and answers the question "In terms of array geometry, is there a specific array or class of arrays that generally outperforms other arrays?".

## 1.2 Thesis Content

This thesis presents results for an investigation into the effects of array geometry on a wireless communications system. The study was performed using simulations of various array

[1] At PCS frequencies (1850-1990 MHz) and higher, multiple antennas are feasible when considering size.

geometries. A simulation tool, the Array Configuration Simulator (ACS) was developed and used in the study.

Chapter 2 presents basic array antenna theory, aspects of beamforming and RF channel concepts. Chapter 3 presents a simulation tool that was developed by members of the Virginia Tech Antenna Group to model array antennas and a wireless communications channel. Chapter 4 presents a set of array antenna geometries that were simulated and gives more specific information on the channel model as it pertains to the simulations. Chapter 4 concludes with a presentaton of the simulation results. The thesis closes in Chapter 5 with a summary of the findings and conclusions about the simulation process.

# Chapter 2

# Array Antenna Simulation Components

This chapter presents necessary concepts for understanding and modeling portions of a wireless communications link. The purpose of this chapter is to bring the reader to a basic understanding of array antennas, adaptive beam forming, diversity combining, the radio channel channel and modeling of these concepts. This chapter also serves to present a framework for an interested individual to pursue more study in any of the topics covered here.

Section 2.1 presents basic antenna element and array theory. The reader will be introduced to the element pattern and array factor, which are necessary concepts for understanding array antenna operation in wireless communications. Array beamforming for the purpose of interference mitigation is an important application of array antennas in wireless communications. Fixed beamforming and adaptive beam forming approaches are presented in Section 2.2. Array antennas can also be designed to provide system diversity. A definition of diversity is given in Section 2.3. Section 2.3 also provides a discussion on the purpose of diversity techniques, and on the methods of diversity combining. Section 2.4 provides a few definitions that are useful in radio channel characterization. More information about the radio channel will be presented in terms of channel modeling concepts in Section 2.5. In Section 2.5, modeling of the free space and multipath environments are discussed. Definitions of flat fading channels and frequency selective channels are also provided. Modeling of scatterers, interference and noise are also discussed in Section 2.5. The chapter concludes with a sum-

mary in Section 2.6. The information contained in this chapter will be used in Chapters 3 - 4 to discuss the development and use of a wireless communication simulation tool.

As presented in Section 1.1 of this thesis, the motivation for this research is to demonstrate the benefit of implementing certain array topologies for enhancing wireless communications system performance. The goal was to ascertain what array topologies outperform other topologies in a general-case, macrocell, wireless, communication link. The simulation criteria of performance used in the simulation campaigns were Bit Error Rate (BER) and array pattern data. For this research, an existing simulation tool, Vector Multipath Propagation Simulator (VMPS), was modified to create the Antenna Configuration Simulator (ACS) (see Chapter 3). The ACS was used to carry out the simulations of a wireless communications system. Specifically, the ACS simulations were conducted to analyze the relative performance of various array antenna configurations. The intent was to determine a best configuration (or topology) for a base station array antenna.

## 2.1 Element Pattern and Array Factors

In wireless communication systems, antennas are the interface between the channel and radio. In choosing antennas for a system, designers must decide whether one antenna used for transmit and receive will suffice or if several antennas must be combined in a feed network to form an array antenna at the transmitter, at the receiver, or both. Deployment of an array antenna is more costly and complex than deployment of a single element. The added complexity and cost may be tolerable when considering the system performance enhancements that can be realized by using an array antenna. Assuming an array antenna is necessary in a particular wireless link, the array designer must choose the array element type and define the array geometry. This research deals with choosing the proper geometry of an array antenna for a wireless communication system. Basic antenna element and array theory are presented in Sections 2.1.1 and 2.1.2, respectively. The reader is referred to the IEEE Standard Definitions [1] for definitions of terms used in this section. The discussion in Sections 2.1.1 and 2.1.2 largely follows that of [2] and [3].

### 2.1.1 Element Pattern

In antenna analysis, the far-field radiation pattern is usually of primary interest. The far-field condition is of interest for analytical purposes and for practical reasons. The analytical aspect will be investigated first, and then the practical aspect will be discused. This section concludes by combining the analytical and practical components of antenna analysis to develop the pattern expression of a $\frac{\lambda}{2}$ dipole element, where $\lambda$ represents wavelength.

#### 2.1.1.1 Simple Electromagnetic Radiation

Starting with basic electromagnetic theory, the static electric field of a hypothetical point charge, $Q$ in free space is given in [4] as

$$\vec{E} = \frac{Q}{4\pi\epsilon_o r^2}\hat{r}. \tag{2.1}$$

In (2.1), $\epsilon_o$ is the permittivity of free space ($\approx 8.85\frac{picoFarads}{meter}$), $r$ is the distance from the point source, $Q$, to the point of observation in the $\hat{r}$ direction and $\vec{E}$ is the electric field in units of $\frac{Volts}{meter}$. In a spherical coordinate system $(r, \theta, \phi)$, it can be seen that the electric field magnitude $E$ has no variation in $\theta, \phi$. The field has $r$ dependence only and decays by a factor of $\frac{1}{r^2}$. This simple field is produced by the simple geometry of the point charge and the uniform distribution of charge on the surface of the point charge. As the point of observation is moved to infinity, from the location of the point charge, $Q$, the spherical field, $\vec{E}$, appears locally at the point of observation, as a planar field that still maintains dependence only upon $r$ and whose magnitude decays as $\frac{1}{r^2}$.

#### 2.1.1.2 Simple Antenna Radiation

In practical antenna analysis, antennas are not point charges. However, by using an alternating current (AC) source to feed an antenna, a distribution of charge can be established on the surface of the antenna. As the current flows onto the antenna, the charge distribution changes with time, thereby creating a distribution of 'point charges' that radiate energy into space.

The spherical to planar field assumption that was used for the electric field of the individual point charge is used in antenna radiation analysis for observations at great distances from

the antenna. This 'great distance', is relative to the antenna dimension and the wavelength of interest. By making the plane wave assumption, the geometry of a radiation problem becomes relatively simple. There is a minimum distance criteria that must be met to discuss radiation in the far-field, and thus, in plane wave terms. The minimum distance is known as the far field (or Rayleigh) distance, $r_{ff}$ [2]. The far-field distance, $r_{ff}$, for an antenna with largest dimension $D$, that is operating at a frequency with wavelength $\lambda$, is given in [2] as

$$r_{ff} = \frac{2D^2}{\lambda}. \tag{2.2}$$

It is important to note that (2.2) is a necessary, but not sufficient condition in establishing the far-field distance for a radiating element. The following two conditions must also be met in conjunction with (2.2), to establish a correct value for the far-field distance [2].

$$r >> D \tag{2.3}$$

$$r >> \lambda \tag{2.4}$$

#### 2.1.1.3 Practical Antenna Application

To show that most practical wireless applications have receive antennas in the far-field of the transmit antenna, an example is given using the UHF band (300 MHz$\leq f_c \leq$3000 MHz).

**EXAMPLE 2-1** ***Far-field criteria for a UHF application***

Consider a simple antenna (e.g. a $\frac{\lambda}{2}$ dipole) for a UHF application. Using $D = \frac{\lambda}{2}$, (2.2) gives $r_{ff} = \frac{\lambda}{2}$. The condition in (2.3) is met for $r >> \frac{\lambda}{2}$. Since the largest wavelength in the UHF band is 1 meter, (2.4) states that the condition $r >> 1$ meter must be met.

Most UHF wireless applications require propagation distances ($r$) on the order of a few kilometers or more. Therefore, the far-field conditions are easily met by the separation of the transmitter and receiver, and the plane wave assumption is considered valid.

#### 2.1.1.4 Antenna Pattern

An antenna (in transmit mode) is said to radiate in a way that can be described by the far-field antenna radiation pattern. The far-field pattern is primarily defined by the antenna element's geometry, and secondarily defined by factors such as the feed (feed method and mismatch factors), the antenna efficiency and environmental conditions (rain, snow ice, etc). Assuming free space conditions near the antenna, a perfect feed match, a 100% efficient antenna with no rain, snow, etc. on the element, the following radiation pattern development is given, following closely with the discussion in [2].

Consider a $\frac{\lambda}{2}$ dipole antenna connected to a coaxial cable carrying a sinusoidal signal. The voltage, $v(t)$ in the cable is said to feed the antenna element and a current distribution will be established on the element. The element, with a radiation resistance, $R_{rad}$, and the time varying current on the element will give rise to a radiated electromagnetic field (see Section 2.1.1.1). The radiated field strength is dependent upon the element shape and the current distribution. It is known that half-wave dipoles have sinusoidal current distributions along the axes of the antennas [5]. The current distribution along the antenna produces a field pattern, $f(\theta, \phi)$, when expressed in spherical coordinates, for a specific $r$. Figure 2.1 shows the radiation pattern of a vertically oriented ideal dipole. Figure 2.1(b) presents the radiation pattern of the dipole in the E-plane. Notice there is dependence only on $r$ and $\theta$, the radial distance from the antenna and the angle from the zenith, respectively. Figure 2.1(c) depicts the omni-directional pattern in the plane parallel to the dipole's axis of symmetry, (i.e. the H-plane). In the H-plane, there is dependence only upon $r$.

An aside is taken to discuss the terms E-plane and H-plane. Each of the respective planes are known as *principal planes* [2] and are used as reference conventions. In the case of a vertically oriented half-wave dipole, the radiation is such that the radiated electromagnetic wave will have a vertically polarized electric field vector. Perpendicular to the electric field vector is the magnetic field vector, which is polarized in a horizontal fashion. The E-plane is that plane in which the electric field vector is contained. The H-plane is that plane in which the magnetic field vector is contained. Using the vertically oriented half-wave dipole as an example, the E-plane is that plane which is vertical (oriented as the dipole is oriented). The H-plane is perpendicular to the E-plane and in the dipole case, is oriented such that it is perpendicular to the antenna. Figures 2.1(b) and 2.1(c) provide a visual representation of

the principal planes (E and H).

Returning to the dipole pattern discussion, it is shown in Figure 2.1(b) that there is dependence on $r$ and $\theta$. Clearly, the radiation pattern in this plane is not omni-directional. The dipole's geometry and current distribution causes the variation in the E-plane and the omni-directional H-plane characteristics of the radiation pattern.

In practice, a physical dipole radiation pattern deviates from the ideal patterns given in Figure 2.1. Approximations are made for calculation purposes and the dipole is assumed to radiate in the $\theta = 90^o$ plane (in a polar coordinate system $[r, \theta, \phi]$) as shown in Figure 2.1(c).

### 2.1.2 Array Factors

An array antenna is formed by connecting multiple antenna elements in a feed network [3]. Far field radiation patterns for array antennas with simple geometries can be easily calculated if mutual coupling can be neglected. Mutual coupling is, in fact, neglected in this treatment of array theory, and the discussion continues under this assumption. The radiation pattern of an array is the product of the *element pattern* as discussed in Section 2.1.1 and the *array factor*, assuming all elements are identical in type and in orientation.

The array factor is developed analytically by replacing all array antenna elements with isotropic radiators. This assumes a transmit mode of operation for the elements of the array. The isotropic radiator can be described by the constant, $I_0$, representing a normzlized current. Similar constants are then used to describe each element in the array factor. In essence, the array factor is merely a description of the location of the elements in the array antenna, and their collective radiation pattern, assuming all elements are isotropic radiators. For the array to operate in receive mode, the array factor for any array is given in [3] as

$$AF = I_0 e^{j\xi_0} + I_1 e^{j\xi_1} + I_2 e^{j\xi_2} + \cdots \tag{2.5}$$

where $\xi_0$, $xi_1$,$\cdots$ are the phases of an incoming plane wave as observed at the respective antenna elements. The terms $I_0$, $I_1$,$\cdots$, which can be complex-valued, provide amplitude weight and phase shift for the array elements. Typically, $I_i$ is given as $I_0 e^{j\theta_i}$. The transmit mode of array operation is very similar, but not given here.

Once the array factor is determined, the element patterns of the actual array antenna elements (e.g $\frac{\lambda}{2}$ dipole) are used to replace the isotropic radiator expression, using pattern

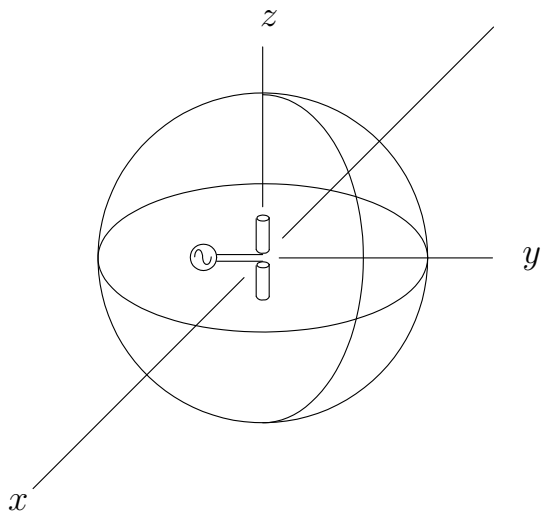


(a) Ideal Dipole

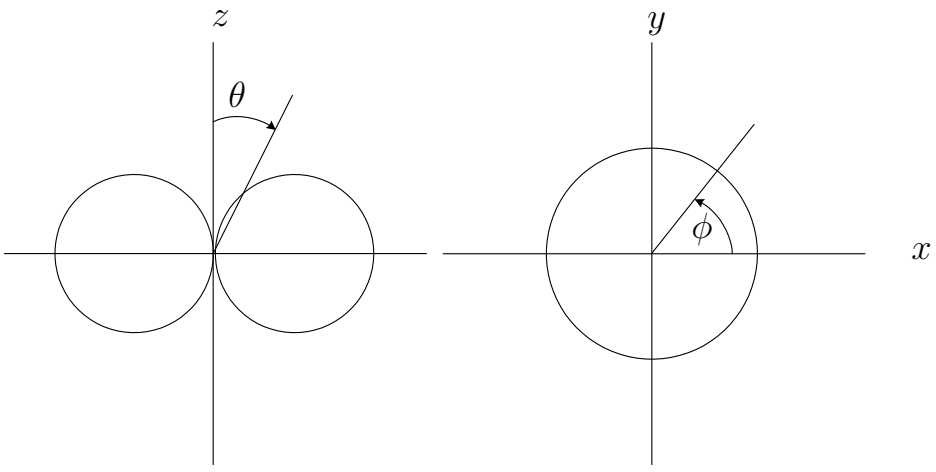


(b) E-Plane Radiation Pattern

(c) H-Plane Radiation Pattern

**Figure 2.1** An ideal dipole and its associated principal plane radiation patterns [2]

multiplication of $AF$ and the element patterns. This provides a more accurate description of each individual element in the array antenna. Each element then can be weighted separately to provide array antenna beam forming.

## 2.2 Array Beamforming

Once the element pattern expressions are calculated, the individual array elements can be weighted in a process known as beamforming to form a specific array factor and resultant array pattern. Figure 2.2 depicts a $k$ element array that implements a beamformer, where manipulation of weights $w_1$ to $w_k$ provide means to form array patterns with specific characteristics. Each of the $k$ elements has an associated weight, $w$. The beamformer diagram shows a summation, $\Sigma$ of all $k$ weighted signals. In practice, the weights $w_1$ to $w_k$ and the summation, can be used to provide fixed or fully adaptive beamforming. The purpose of beamforming and the classifications of beamforming (fixed and fully adaptive) will be discussed in Sections 2.2.1 and 2.2.2.

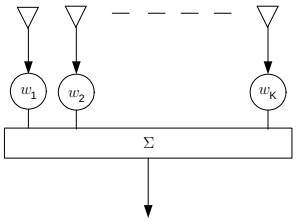


**Figure 2.2** Block diagram of a beamformer for a $k$ element array

### 2.2.1 Purpose of Array Beamforming

As alluded to in the previous paragraph, individual array elements can be weighted. This weighting process enables an array system to steer beams, produce nulls, etc., to enhance the link in a wireless communications channel. Beamforming is primarily used to mitigate interference by producing pattern nulls in the direction of an interferer.

For the case of multipath components present in the system, beamforming is more than a strict geometrical problem. With multipath present, the effects of any signal (desired or

interferer), may sum in a way that would present the transmitter as if it were in a location other than its actual position. Therefore, the beamformer responds to the effects of incoming signals (assuming receive mode), the associated multipath and any system or channel noise that is present.

The approaches to implementing beamformers in an arrayed system are presented in the following sections.

### 2.2.2 Beamformer Classifications

There are various beamforming methods in practice today. These methods can be classified under two major categories, the *fixed beamformer* and the *fully adaptive beamformer*.

#### 2.2.2.1 Fixed Beamforming

A fixed beam steering mechanism weights the elements of an array antenna to provide a specific pattern. This pattern can be specified, within physical constraints, to provide coverage of a specific area. Fixed beam antennas can establish one pattern for the array, or individual beam patterns can be switched to provide improved coverage by the array.

#### 2.2.2.2 Fully Adaptive Beamforming

A fully adaptive array provides a means for beam shaping in any direction, not just over a set of pre-defined directions. Where a switched fixed beam system has pre-defined "look directions" to choose from, an adaptive beam system also provides coverage for areas that would be in between the fixed beam "look directions". Optimum (or optimal) beamforming is, as its name suggests, the best possible solution to a beamforming problem. The adaptive beamformer provides an iterative approximation to the optimal beamformer solution [6]. The optimal solutions are approxmated using algorithms. Much algorithm work has been published in the open literature under the names *adaptive beamforming algorithms*, *adaptive beamforming*, *beamforming algorithms*, etc.

As alluded to earlier, the maximum directive gain is not necessarily in the direction of the desired user. In addition, the nulls are not necessarily positioned directly toward the

interferers. An adaptive beamformer, with the use of an adaptive algorithm and hardware, properly weights each antenna element within the array so as to provide a best response for the array. The weight, or multiplier of each antenna is used so that the collective response of each antenna yields a useful array response for the particular scenario.

There are many beamforming algorithms (techniques) that are in the open literature. The algorithms are used to calculate array weights, based upon some criteria. Three such criteria are presented in [7] as the Minimum Mean Square Error (MMSE) algorithm, the Maximal Signal to Interference plus Noise Ratio (Max SINR) criterion and the Minimum Variance (MV) criterion. A variation of the Minimum Variance is the Linearly Constrained Minimum Variance (LCMV), and is also presented in [7]. For the purposes of this thesis, MMSE will be further explained in Chapter 3.

This portion concludes the information on array beamforming. The next section of this chapter will deal with array diversity and diversity combining.

## 2.3 Diversity and Diversity Combining

Reflections and scatterering in a channel give rise to the creation of multipath signal components. Signal amplitudes, signal phases, and times of arrival for the multipath signal components are different from that of the line of sight (LOS) components. Within a group of multipath components, various amplitudes, phases and times of arrival are present at the receive antenna. Delay spread, angle spread, power delay profile, etc., are a few terms that are used to describe the multipath characteristics of a channel. Signal fading can be caused by the various signal components (LOS and/or multipath) summing to cancel the signal. This type of fading is known as multipath fading. The purpose of implementing diversity with receive array antennas is to combat the multipath fading. One portion of the diversity topic is the study of the combining methods. That is, once diversity is built into a system through polarization, angle or spatial techniques, how does one combine the information properly to maximize the signal to noise ratio (SNR)?

### 2.3.1 Diversity

In [8], a high level definition of diversity is given as:

> "Diversity is achieved by using the information on the different branches available to the receiver in order to increase the signal-to-noise ratio at the decoding stage. Having additional branches increases the probability that at least one branch, or the combined branch outputs, produces a sufficiently high SNR to permit reliable decoding of the message at the receiver." [8]

Greatly delayed multipath components of the desired user can be considered to be interference. According to [8], a rule of thumb can be applied to determine whether or not multipath might cause interference. More will be said about this in Section 2.4. When multipath acts as interference, the diversity techniques (used to combat multipath fading), might not be as effective. In this case, beamforming techniques would be used to null the source of interference, thereby eliminating that component of signal diversity. Therefore, one must be careful in describing the channel effects on a signal when discussing diversity and diversity gain.

### 2.3.2 Combining

After establishing system diversity branches by varying antenna placements, polarization, etc., the diversity branches must be combined to yield a signal that overcomes fading. Three particular combining techniques of interest are *selection*, *equal gain* and *maximal ratio* combining. These techniques are methods of summing energy received by an array antenna. The algorithms are combining schemes that take advantage of system diversity. Following closely with the discussion in [9], the three combining techniques are presented as follows.

Selection combining is the simplest of the three combining techniques presented in this thesis. For a selection combiner, all antenna elements can be monitored simultaneously, and the antenna element with the highest signal-to-noise ratio, (SNR) is chosen, or selected, to provide the array output. A representation of selection combining is given in Figure 2.3(a). An Equal Gain Combiner (see Figure 2.3(b)) is a little more complex than the Selection Combiner. In Equal Gain combining, "The signals on each antenna are combined by bringing all phases of the signals to a common reference point (cophasing). That is, the combined signal is the sum of the instantaneous fading envelopes of the individual branches..." This sum then is used as the input to the signal processing decision making process. Equal Gain, as stated in [10], is a variation of Maximal Ratio Combining. The Maximal Ratio Combiner (see Figure 2.3(c)) also weights all branches, similar to the Equal Gain Combiner, but each branch

is weighted with respect to the instantaneous carrier-to-noise ratio (CNR) [9]. Then, each branch is cophased and summed as in the Equal Gain combining scheme. In Figure 2.3(c), there is a connection between the antenna element output and the weighted output. This connection represents the measurement of the instantaneous CNR of the antenna element that is then used to calculate the weight and phase for the antenna element. The weighted elements are then cophased, summed and used as input to the rest of the system. It is important to note that Maximal Ratio Combining is the most complicated of the three combining techniques presented here, but it does take the most advantage of the diversity branches in the system. For a more thorough treatment of diversity and diversity combining, the reader is referred to [6–9].

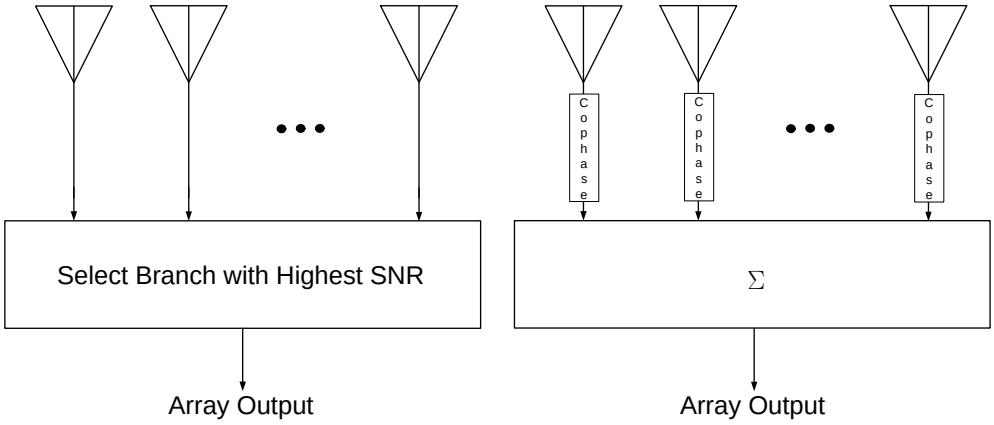


(a) Selection Combiner

(b) Equal Gain Combiner

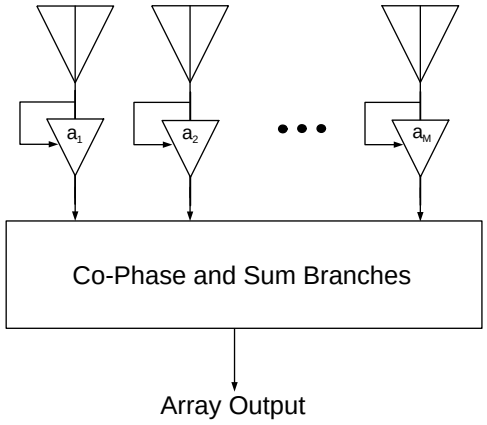


(c) Maximal Ratio Combiner

**Figure 2.3** Block diagrams of the Selection, Equal Gain and Maximal Ratio Combiners.

## 2.4 Radio Channel

In broad terms, a radio channel is any path through which RF energy passes to complete a transmit/receive circuit. In the channel, or environment, characteristics of a transmitted electromagnetic wave are altered by such phenomena as fading, interference, propagation (path) loss, etc. Channel environments can be categorized and described as given in Table 2.1. Figure 2.4 presents graphical representation of the channel environment categories listed in Table 2.1. The free space channel is ideal. In practice, multipath is present due to objects within the channel, and interference is often a factor. Large obstructions in a channel obstruct the LOS path of propagation, thereby creating a NLOS channel, as represented in Figure 2.4(d).

A radio channel is largely distinguished by the amount of inter-symbol interference (ISI) it introduces and by how fast the channel changes with time [8]. Weather changes and movement of the transmitter, receiver and/or objects within a channel will cause the channel to vary over time. ISI is introduced by multipath signal components that are significant in amplitude and are delayed in time $\geq \frac{1}{10}$ of a symbol duration from the primary signal component [8]. Multipath components that arrive within $\frac{1}{10}$ of a symbol duration of the primary signal component, do not cause ISI, but can cause multipath fading. These deleterious effects (ISI and multipath fading) on the signal of interest must be overcome to provide reliable wireless communications. To that end, adaptive beamforming algorithms and diversity combining algorithms are developed. Siting of transmit and receive antennas are important. Power requirements also are of major concern. Modulation schemes can also have inherent characteristics that provide better or worse performance for a wireless communication system. All of these issues and many more are considered in a wireless system development and deployment.

**Table 2.1** Categorization of Channel Environments

| Category | Objects in Channel? | LOS/NLOS | Fading | Figure |
|---|---|---|---|---|
| Free space | No | LOS | flat fading | 2.4(a) |
| LOS Multipath Environment | Yes | LOS + NLOS | flat fading or frequency selective | 2.4(b) |
| LOS Multipath + LOS Interference | Yes | LOS + NLOS | flat fading or frequency selective | 2.4(c) |
| NLOS Multipath | Yes | NLOS | flat fading or frequency selective | 2.4(d) |

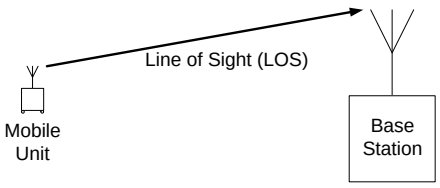


(a) Free Space Channel Environment

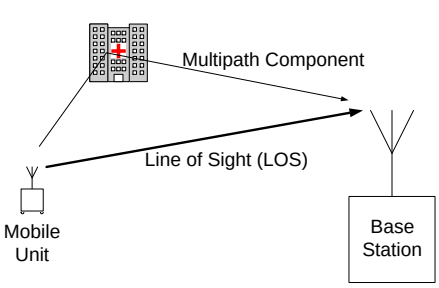


(b) Multipath Channel Environment

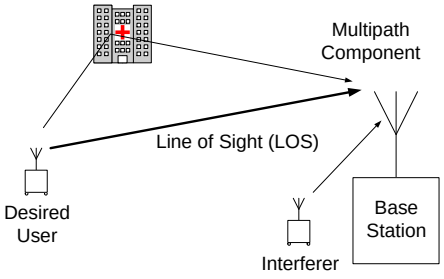


(c) Channel Environment with Multipath and Interference

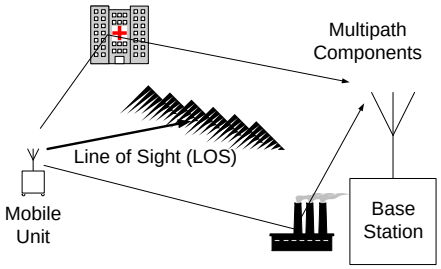


(d) Non-Line of Sight Channel Environment

**Figure 2.4** Illustrations of common propagatic channel environments

## 2.5 Channel Modeling

To enhance deployment, optimization and maintenance of wireless systems, channel models have been developed to analyze propagation and transmit/receive effects in a channel. Channel models are analytical tools that give system designers insight to effects on a proposed system; an overview of spatial channel models is presented in [11]. According to [11], a spatial channel model builds upon classical channel model fundamentals and include such things as time delay spread, angle of arrival (AOA) and adaptive array antenna geometries. The channel model should consider transmit power, transmit and receive antenna locations, scatterers/multipath affects and interference, among other factors. Channel models are typically comprised of submodels (or model components) of the individual channel characteristics to create the overall model that describes the wireless channel. Some aspects of channel modeling are presented in the following Sections 2.5.1 - 2.5.5.

### 2.5.1 Free Space

A channel can be modeled as a free space or a multipath environment. A free space environment is an environment in which no multipath and no obstructions exist. The equation governing the propagation path loss in a free space environment is known as the Friis Transmission Formula, and is given by (2.6).

$$P_{Rx} = G_{AT}\Big(\frac{P_{Tx}}{4\pi r^2}\Big)(A_{eR}) \tag{2.6}$$

In (2.6) $P_{Rx}$ denotes received power, and $P_{Tx}$ denotes transmitted power. The distance of propagation is given as $r$. $G_{AT}$ is the gain of the transmit antenna. $A_{eR}$ is the effective area of the receive antenna. The received power decays by the factor $r^2$.

### 2.5.2 Scatterers

The presence of objects in a channel cause the channel to lose its 'Free Space' classification. When this occurs, various methods of propagation take place. Direct propagation, reflection, diffraction and scattering are the four main propagation mechanisms according to [7]. This

thesis focuses on direct propagation (LOS signal components), reflection and scattering. [1] For modeling purposes, direct propagation can be viewed as free-space propagation. The effects of propagation due to reflection and scattering are then 'added' to the direct (LOS) propagation components to give a more complete picture of propagation phenomena.

Reflection and scattering, two different phenomena, are functions of two factors, the wavelength and the object dimensions. For a propagating wave to reflect from an object, the wavelength is typically small in comparison to the dimensions of the object [7]. For scattering to occur, the dimensions of the object are typically small in comparison to the wavelength of interest [7]. Small objects and rough surfaces can cause scattering. Reflections and scattering cause multipath in a channel. For the purposes of this thesis, reflection and scattering are treated as the same phenomena and given the term scattering.

Objects that reflect or diffract electromagnetic energy give rise to scattering of an electromagnetic wave. Some examples of scatterers that are present in the physical world are buildings, vehicles, lamp posts and bodies of water. If a channel gives rise to multipath signal components, then the channel is not properly described by just the Friis Transmission formula of (2.6). To compensate for the deviation from (2.6), channel models can be developed to model propagation in this type of environment.

In the open literature, many scatterer models are presented that can be used to describe the scatter effects within the channel. Vector propagation channel models are used to predict the performance of wireless systems [7]. A single bounce model accounts for multipath components that interact with only one scatterer then propagate to the receiver. Direct straight line propagation between two points of interest (i.e. ray-tracing), is often used in simulation to describe the single bounce multipath propagation. Single bounce is not what happens in the physical world, but it is a useful technique for an initial approximation.

A visual example of three vector propagation channel models is given in Figure 2.5. In Figure 2.5(a), a representation of the Lee Scatterer Model, it is shown that the scatterers are placed equidistant to the transmitter. All scatterers have direct paths from the transmitter and to the receiver. According to [11], the scatterers in the Lee Model "...are intended to represent the effect of many scatterers within the region, and hence are referred to as *effective scatterers*.". Notice that in Figure 2.5(a), the base station is considered to be two antenna

[1] For a treatment of diffraction, the reader is referred to texts on radio wave propagation, electromagnetic theory and antenna theory. Examples of such texts are: [12–14]

elements separated by a distance $d$. The Lee model was originally used to predict the signals received by two sensors as a function of element spacing [11]. The authors of [11] conclude that the Lee Model is useful in analyzing the correlation of received signals at two separated sensors, but it is not well suited to completely model the wireless channel.

In **??**, a representation of the geometrically-based, single-bounce, elliptical model (GBS-BEM), it is shown that scatterers are randomly placed in an elliptical region surrounding the mobile and base station. According to [11], the mobile and base stations are at the foci of the ellipse in the Elliptical Model. The model was created to describe the microcell environment, where it is common for scatterers to be surrounding the mobile and base stations. The constraint on the scatterer locations for both the Lee and Elliptical models is a parameter that establishes the maximum separation of a scatterer and the point of interest, on a time scale. This separation defines the delay spread limit within the channel. The maximum time, $\Delta\tau_{max}$ is established using (2.7), where $d_{max}$ is the maximum distance from any scatterer to the point of interest, and $c_o$ is the speed of light (speed of an electromagnetic wave propagating in free space). It is interesting to note that the total distance from one foci to the other foci via the ellipse boundary is a constant for a particular ellipse. This total distance is the maximum distance a multipath signal component will travel in the elliptical model. One last detail about the Elliptical Model is that this model is also known as the Liberti Model [7]. A third scatterer model, as presented in [7], is the Uniform-Sector Model or Norklit's Model. Figure 2.5(c) shows a representation of the Uniform Sector Model. The Uniform Sector Model assumes that the reflection coefficients of scatterers are uniformly distributed in magnitude over [0,1] and in phase over [0,2$\pi$]. Additionally, the scatterers are assumed to be uniformly distributed in an angular range, $\Delta\phi$, and radial distance $\Delta r$ [7], centered about the mobile station.

$$\Delta\tau_{max} = \frac{d_{max}}{c_o} \tag{2.7}$$

### 2.5.3 Bandwidth Effects

Frequency effects of fading must also be considered when modeling a channel. A wireless channel can be described as a flat fading channel or it can be described as a frequency selective channel. A channel is said to experience flat fading if all frequencies of interest propagate

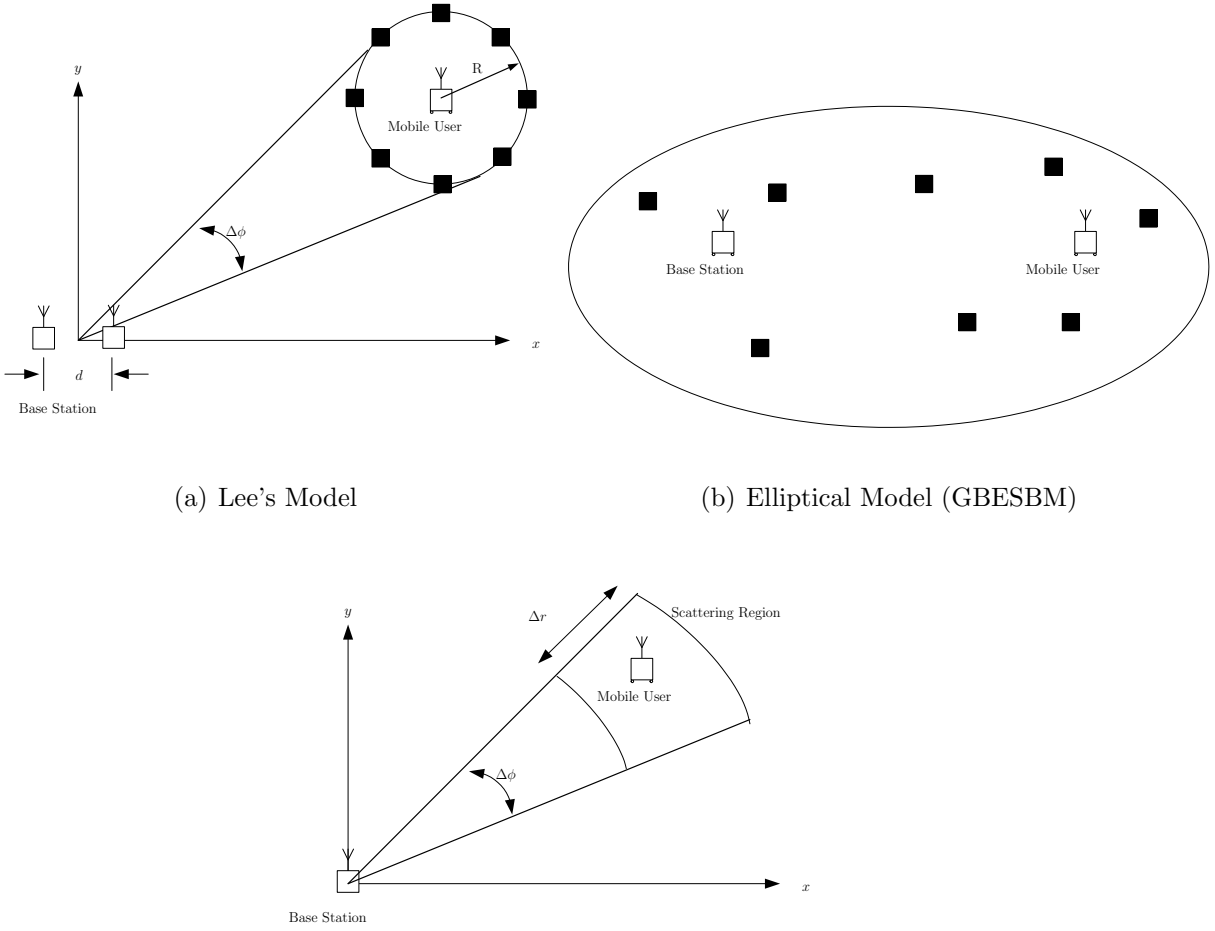


(a) Lee's Model

(b) Elliptical Model (GBESBM)

(c) Uniform Sector Model (Norklit's Model)

**Figure 2.5** Graphical representation of three vector propagation channel models [7].

in the same manner through the channel. That is, all frequencies of interest fade equally. Free space is a flat fading channel. For many narrowband transmissions (e.g. bandwidths on the order of a few hundred Hz), channels often respond in a flat fading manner. For wideband transmissions, the channel can respond quite differently for various frequencies contained in the signal. For a wideband signal, the various frequency components might interact with the channel to provide various delays. More importantly, certain frequencies within the bandwidth of interest will undergo more attenuation than other frequencies in the bandwidth. This attenuation of the signal is typically caused by multipath and LOS signals of certain frequencies adding destructively at the receiver.

### 2.5.4 Interference

Modeling of interference is also of great importance when describing a wireless channel. Interference is predominately caused by undesired users in the system, as stated in Section 2.4, but it can also come from the multipath of the desired user's signal. Thus, it can be said that if conditions are right, a user can be its own interferer. This phenomena occurs when the multipath components are greatly delayed, yet strong in amplitude relative to the LOS component. The amount of delay and the strength of the component are what determine whether or not the multipath component is considered to be interference. As delayed multipath signal components arrive $\frac{1}{10}$ of a symbol duration or later, with signal amplitudes comparable to that of the LOS component, the signal acts as interference [8]. Therefore, if channel conditions produce delayed, yet stong multipath components, a desired user can act as its own interferer.

### 2.5.5 Noise

In a real, physical channel, noise is always present. Noise is usually considered to be an undesirable quantity in a channel. Noise sources can be considered correlated or uncorrelated. There are predominately two classifications of noise, thermal noise and noise due to other sources (interferers, multipath, jammers, etc.). According to [15], thermal noise is produced by the random movement of free electrons in conductors and semiconductors. This noise is 'white' (i.e. present at all frequencies) and the white noise power can be reduced, though

never eliminated, in a system by decreasing bandwidth and decreasing the noise temperature of the RF and antenna hardware. Interferers or jammers, and multipath also introduce noise into a system.

There are certain techniques that can be used to successfully communicate in noisy environments. Multiple access schemes and modulation techniques can be used to limit noise power within the frequency band of interest. In an environment with spatially correlated noise, beamforming techniques can be applied to null interferers and/or certain multipath components to provide a 'quieter' environment.

## 2.6 Summary

This chapter discussed basic concepts in element and array theory, beamforming, diversity and channel modeling. In Section 2.1, basic antenna element and array theory was presented. In section 2.2 beamforming concepts were presented. Receive antenna diversity was presented in 2.3. The chapter continued with a discussion of an RF channel and some of its characteristics in Section 2.4. Modeling of the radio channel and more channel theory was presented in Section 2.5. This chapter does not provide an exhaustive review of antennas, arrays, radio channels and diversity mechanisms, but does address highlights of these issues. The writing in this chapter provided some insight to many topics. It is hoped that the reader has a better understanding of the wireless channel and components of a channel that must be considered in creating models for simulation of wireless communication links.

# References


[1] Antenna Standards Committee of the IEEE Antennas and Propagation Society, Piscataway, NJ, *IEEE Standard Definitions of Terms for Antennas*, 145-1993 ed., 1993.

[2] W. L. Stutzman and G. A. Thiele, *Antenna Theory and Design*, ch. 1. John Wiley & Sons, Inc., 2 ed., 1998.

[3] W. L. Stutzman and G. A. Thiele, *Antenna Theory and Design*, ch. 3. John Wiley & Sons, Inc., 2 ed., 1998.

[4] J. D. Kraus and D. A. Fleisch, *Electromagnetics with Applications*, ch. 2. McGraw-Hill, 1999.

[5] W. L. Stutzman and G. A. Thiele, *Antenna Theory and Design*, ch. 2. John Wiley & Sons, Inc., 2 ed., 1998.

[6] C. B. Dietrich, Jr., *Adaptive Arrays and Diversity Antenna Configurations for Handheld Wireless Communication Terminals*. PhD thesis, Virginia Tech, Blacksburg, VA, February 2000.

[7] B. ki Kim, *Smart Base Station Antenna Performance for Several Scenarios - an Experimental and Modeling Investigation*. PhD thesis, Virginia Polytechnic Institute & State University, Blacksburg, VA, May 2002.

[8] K. P. Dietze, "Analysis of a two branch maximal ratio and selection diversity system with unequal branch powers and correlated inputs for a rayleigh fading channel," Master's thesis, Virginia Polytechnic Institute & State University, Blacksburg, VA, March 2001.

[9] J. Litva and T. K.-Y. Lo, *Digital Beamforming in Wireless Communications*. Boston, London: Artech House, 1996.

[10] K. P. Dietze, "Vector Multipath Propagation Simulator." VTAG Internal document, May 1999.

[11] R. B. Ertel, P. Cardieri, K. W. Sowerby, T. S. Rappaport, and J. H. Reed, "Overview of spatial channel models for antenna array communication systems," *IEEE Personal Communications*, pp. 10–22, February 1998.

[12] J. D. Kraus and D. A. Fleisch, *Electromagnetics with Applications*. 1999.

[13] S. Ramo, J. R. Whinnery, and T. V. Duzer, *Fields and Waves in Communication Electronics*. John Wiley & Sons, Inc., 3 ed., 1994.

[14] W. L. Stutzman and G. A. Thiele, *Antenna Theory and Design*. John Wiley & Sons, Inc., 2 ed., 1998.

[15] N. Paul Denzer, ed., *The ARRL Handbook*. Newington, CT: The American Radio Relay League, 74 ed., 1997.

# Chapter 3

# The Array Configuration Simulator

The Array Configuration Simulator (ACS) is a simulaton tool that can be used to model a base station array and mobile users in a wireless channel. ACS is a modification of the Virginia Tech Antenna Group's Vector Multipath Propagation Simulator (VMPS). A brief comparison of VMPS and ACS is given in Section 3.1. The rest of the chapter will be solely devoted to the discussion of ACS. In Section 3.2, an overview of ACS is given. The overview includes a high-level explanation of the execution of an ACS simulation. It also includes an introduction to the types of analyses that can be performed using ACS. Section 3.3 discusses the specifics of the transmitted signal that is employed by the simulator. Sections 3.4 and 3.5 focus on the specific beamforming algorithm and diversity combiner implemented in ACS. A significant portion of this chapter is devoted to the ACS channel model. The channel model is presented in Section 3.6. Results from two selected simulations are given in Section 3.7, merely to provide the reader with an idea of the capabilities of ACS. The chapter concludes with a summary in Section 3.8.

## 3.1 VMPS and ACS

The Vector Multipath Propagation Simulator (VMPS) is a MATLAB based simulator that can be used to simulate certain aspects of a wireless communication system. Its Graphical User Interface (GUI) features enhance the simulator engine capabilities to provide a user friendly simulation environment. According to [1], VMPS "was developed to be used

in conjunction with experimental measurements in either narrowband or wideband signal environments."

Some of the capabilities of VMPS include simulation of "adaptive spatial array and spatial temporal arrays and study their performance under various channel conditions." [1]. Three separate diversity combiners (Selection, Equal Gain, and Maximal Ratio) can also be implemented and their performance can be analyzed. One can also analyze interference rejection capabilities of arrays using VMPS. A wireless communication channel can be defined by selecting a multipath model, positioning transmitters and scatterers, and by setting parameters for movement of the receive array or the system transmitters. All of this can be selected or defined by the user using the VMPS GUI.

The purpose of developing and using ACS was to provide a means of comparing relative base station array performance for user-defined array geometries. Similar to VMPS, the ACS software enables a user to specify many parameters to simulate a wireless communications channel. Both simulators can perform a Bit Error Rate (BER) computation and provide antenna pattern plots and pattern data.

ACS differs from VMPS in that ACS used one specific diversity combiner (Maximal Ratio), it implemented spatial arrays only and the ACS simulator was not developed in conjunction with experimental measurements.

## 3.2 Overview of ACS

The basic order of operations in simulating a wireless communication link using ACS is presented in Figure 3.1. In Figure 3.1, it is shown that array antenna geometries are selected first. Various geometries can be created by defining the two-dimension Cartesian co-ordinates for each antenna element location. It is important to note that ACS is a two dimensional simulator, all the arrays are planar, with the transmitters and scatterers in the same plane as the array (i.e. azimuth plane, $\theta = 90^o$) and each antenna element is simulated as a vertically oriented dipole. After the array elements are positioned, the user then creates the channel model by defining parameters for line-of-sight(LOS)/non-line-of-sight(N-LOS) conditions, the number, location and power of transmitters, the number, location and reflection coefficient of scatterers, the desired $\frac{E_b}{N_o}$, etc. A bit error rate (BER)

calculation can be performed, and/or a pattern analysis can be performed, depending upon the user-specified type of analysis.

After a simulation set has been defined and the simulation(s) conducted, the user then analyzes the results. The results, as previously stated, can be in the form of a Bit Error Rate (BER) computation or in the form of array pattern data. Regardless of the selected output format, the user analyzes the data and then chooses a better (or best) array from the original set for the application. Figure 3.1, depicts two arrays in the simulation set. Using ACS, the user would be able to choose the better array for his/her specific application.

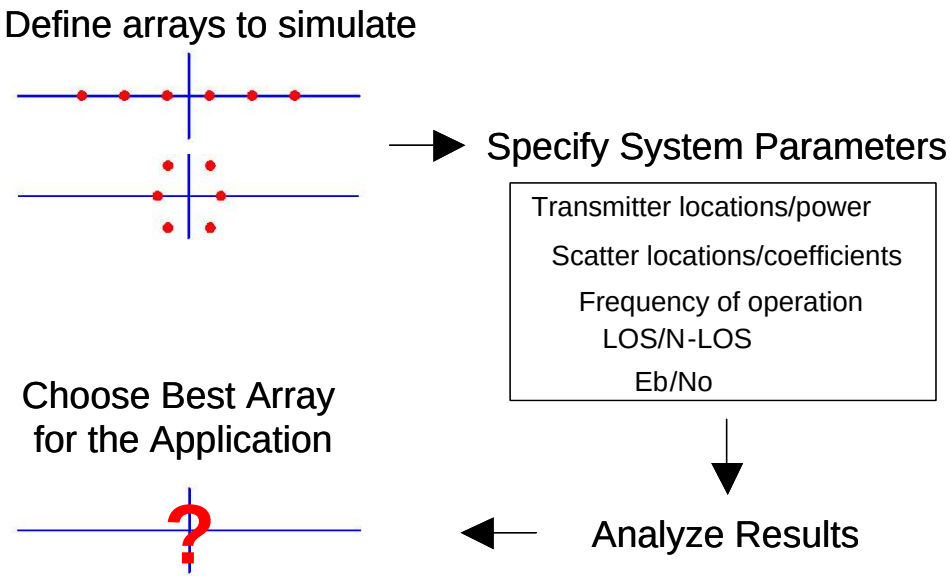


**Figure 3.1** Block Diagram depicting the order of execution for ACS

## 3.3 The Transmitted Signal

The effects of the channel on a transmitted signal were discussed in Section 2.4. Earlier in Chapter 2, the discussion was about beamforming and receiving a signal using an array antenna. The question arises, "What is the signal that is being transmitted in the simulations?". Simply put, the signals being transmitted are wideband (5 MHz) digital signals. More specifically, each transmitted signal is comprised of a random bit stream. The desired user and all interferers transmit the same type of bit stream. Because each transmitter is producing a random bit stream, the transmitters are assumed to be uncorrelated. The carrier frequency can be chosen by the user to meet simulation needs. Binary Phase Shift Keying (BPSK) modulation is used.

The ratio $\frac{E_b}{N_o}$ has been used in this thesis, and is explained here further, as it relates to the transmitted signal. As presented in [2], $\frac{E_b}{N_o}$ is the ratio of the energy per bit $E_b$, to the noise Power Spectral Density, $N_o$. Discussed in terms of dB, this value is used to characterize the noise in the system as it relates to the desired user's signal. In the simulations, $E_b$ is the energy per bit of the desired user's signal only. The user of ACS specifies the $\frac{E_b}{N_o}$ ratio in decibels. The position of the desired user establishes the path loss that will occur from the

desired user to the receive array. The energy received ($E_b$), at the receive array, from the desired user is measured and the $N_o$ value is then calculated to maintain the user defined $\frac{E_b}{N_o}$ ratio for the system. The $E_b$ value describes the energy per bit that is received from the desired user only. The $N_o$ value sets the noise PSD for the entire system. Other transmitters (undesired users) in the system transmit and their respective $E_b$ values are determined by their locations and the associated path loss, as is the case for the desired user. As discussed, $N_o$ is fixed for the entire system. An undesired user might have significantly different $\frac{E_b}{N_o}$ ratios from the desired user and other undesired users. If an undesired user is closer to the receive array than the desired user, it will cause a significant interference problem for the array. If, however, an undesired user is farther away from the receive array than the desired user, it might create minimal or no interference at the receive array.

## 3.4 The ACS Beamformer

One aspect to consider for a base station array is the beamformer algorithm. The purpose of the beamformer is to enhance the array's ability to collect the desired user's signal, while mitigating interference. In theory, an optimal beam former should be implemented at the receive array. The weights provided to the receive array elements by an optimal beamformer would provide the best solution for the array. In practice, adaptive beamformers are employed to find the optimal beamformer solution. Adaptive beamforming algorithms iteratively provide approximations of the optimal beamformer solution. The array responds to an incoming signal based, in part, on the adaptive beamformer's ability to beamform on the desired user while mitigating any interference. Naturally, the response of the array is limited to the robustness of the adaptive algorithm and the receive array topology (number and type of elements, geometry, etc.).

The ACS software implements the Minimum Mean-Square Error (MMSE) criterion for the adaptive beamformer. A beamforming algorithm is used to create weights for the array elements that minimize the mean-square error (MSE) between the beamformer output and the reference signal [3]. The received signal, $\mathbf{u}(t)$ is weighted by the Hermitian weight matrix $\mathbf{w}$ and compared to the known training signal, $d(t)$ to determine the error, $e(t)$. The mean-square error is determined by [4]

$$E[e^2(t)] = E[|d(t) - \mathbf{w}^H \mathbf{u}(t)|^2] \tag{3.1}$$

In (3.1), $E[x]$ signifies the expected value or *mean* of the set $x$.

In practice, the weights are updated periodically to adapt to the changing environment. The changes in the environment are due to such things as a change in the number of users, and/or a change in the position and speed of users within the system. The reference signal can be contained in a message header, or in a pilot tone in deployed wireless systems.

## 3.5 The ACS Diversity Combiner

The Maximal Ratio Combining scheme is implemented by ACS. For a situation with no interference the Maximal Ratio Combiner (MRC) provides the optimal solution. The reader might recall that in Section 2.3, MRC was discussed in conjunction with other diversity combining techniques.

## 3.6 The ACS Channel Model

The channel model implemented in ACS is discussed in two parts. The first part, Section 3.6.1 details the construction of the basic model. That is, the way in which the channel affects a signal and how the effects are computed, is established. The second portion of this discussion, in Section 3.6.2 presents the scatterer model and the positioning of transmitters in a simulation. Keep in mind that in Chapter 4 more discussion will be given about the channel model as it was altered for the specific simulations presented therein.

### 3.6.1 The ACS Channel Model Construction

The simulated channel must be constructed so that effects such as multipath, noise, etc. upon a signal can be computed for simulation purposes. It is important to note that this portion of ACS was unaltered in its transformation from the VMPS software mentioned in Section 3.2. Following closely with the discussion in [1], the ACS channel is explained using filter theory.

A radio channel, or environment, can be modeled as a time-varying filter [1]. The array antenna in an environment with one or more transmitters can be modeled as a series of filters as shown in Figure 3.2. In Figure 3.2, the transmitter is 'connected' to each antenna element in the recieve array through the implementation of an impulse response that is particular to that path in the radio channel. Figure 3.2 also depicts an MRC diversity combiner as discussed in Section 2.3.2.

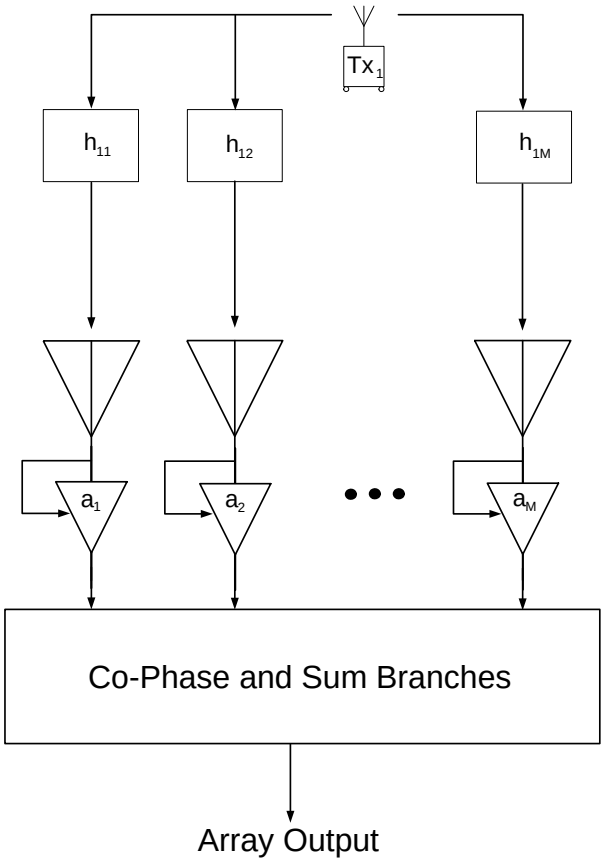


**Figure 3.2** The ACS radio channel is constructed using basic filter theory.

### 3.6.2 ACS Channel Model Content

The contents of the ACS channel model can include a receive antenna array, transmit antennas, and scatterers. The receive antenna array has been discussed in Chapter 2. The beamforming algorithm and diversity combiner implemented in ACS have been discussed in

Sections 3.4 and 3.5, respectively. The transmit antennas and scattering objects, as part of the channel, need to be discussed. First the transmitters are presented, then the scattering model is presented.

#### 3.6.2.1 Transmitters

The following information is specified for each transmitter implemented in ACS: position $r$, zenith angle $\theta = 90^0$, azimuth angle $\phi$; power $P_{Tx}$, and number of associated scatterers, $numScat$. Scatterers are discussed in the following section.

The position of each transmitter can be specified by the user of ACS. Two separate methods of positioning the transmitters were used in the simulations for this thesis. The first method, constrained transmitters to be within a specific range from the receive array (e.g. $300m \leq r \leq 3000m$) and each transmitter was constrained to be within a specific azimuth range of angles, such that each azimuth 'sector' was equal to $\frac{360^o}{num_{tx}}$, where $num_{tx}$ is the number of transmitters in the channel. This method usually ensures that the transmitters are separated in azimuth angle.

A second placement method constrained the transmitters to the same radial distance as stated in the previous paragraph (i.e. $300m \leq r \leq 3000m$), but the transmitters were no longer placed in azimuth sectors. This second method allowed users to be very close in azimuth angle, where the first method allowed at most, only two transmitters to be close in azimuth. Both methods used a MATLAB function, $rand()$ to create position coordinates, within the described constraints. Each transmitter 'scenario' that was created was used for all of the simulated arrays, to provide a means to test relative array performance. When a second set of simulations were conducted, new locations were derived from the $rand()$ function and the prescribed placement constraints.

As discussed in Section 3.3, the transmitters employ the BPSK modulation scheme. In addition, each transmitter generates its own stream of bits, independently of the other transmitters. As will be discussed in Section 4.3.1, this independence has an impact on the type of multipath that is produced.

#### 3.6.2.2 Scatterers

The scatterers are very similar to the transmitters, from the simulation point of view. The scatterers are positioned in sectors as are the transmitters. The scatterers 'transmit' (i.e. reflect) the same data that the transmitters transmit. The scatterers, however, use a reflection coefficient $\Gamma$, in place of the transmitter power term. Also in contrast, scatterers are positioned relative to a transmitter, instead of relative to the receive array. Variables in the ACS software can be set to specify positioning constraints for the scatterers, as was the case for the transmitters. As in the transmitter case, the scatterers can be constrained to azimuth sectors and radial ranges, or they can be allowed to be randomly placed with no sectorization, thereby permitting clusters of scatterers to occur in the simulation.

## 3.7 The ACS Outputs

The user executes the program after defining the array geometries and the channel parameters. The resultant simulation data can be output using one of two specicified formats, namely a Bit error rate (BER) format or a pattern analysis format. The two analysis methods are explained in detail in the following sections. The reader is reminded that more extensive simulation results and data will be given in the following chapter.

### 3.7.1 Bit Error Rate Analysis

An example of output information from an ACS BER analysis is given in graphical form in Figure 3.4. The specific simulation scenarios that give rise to the data are discussed in the following paragraphs.

The BER analysis was a comparison of a six element Uniform Linear Array (ULA) and a six element Uniform Circular Array (UCA) (see Figure 3.3) under the same conditions. The $\frac{E_b}{N_o}$ ratio was set equal to 6 dB. There were five interferers and one desired user in the system, for a total of six users. Each of the users were of the same power and were constrained to be in the region defined by $300m \leq r \leq 3000m$, with no sectorization of the transmitters in the azimuth plane. Each user was surrounded with 6 scatterers, all with a reflection coefficient of $\Gamma = 0.5$. The scatterers were 'sectorized' with one scatterer per $60^0$ of azimuth angle. Each

scatterer was randomly placed (relative to the transmitters) within a radial distance range based upon the frequency of interest. For this simulation, the frequency, $f$, of 2 GHz was implemented, which corresponds to a wavelength, $\lambda$, of 0.15 m. The range over which the scatterers were positioned was $10\lambda \leq r_{scat} \leq 1000\lambda$, or $1.5m \leq r_{scat} \leq 150m$. This results in a scatterer model that assumes scatterers are local to the transmitter. The parameters for this simulation are presented in Table 3.1.

**Table 3.1** Parameters for a BER analysis used to show capabilities of ACS

| Variable | Value | Description |
|---|---|---|
| $N$ | 6 | Number of antenna elements in each receive array |
| $\frac{E_b}{N_o}$ | 6 dB | see Section 3.3 |
| $numTx$ | 6 | Number of transmitters in the system |
| $Txdist$ | [300, 3000] meters | Radial distance of transmitters from receive array |
| $numScat$ | 6 | Number of scatterers per transmitter |
| $freq$ | 2 GHz | Frequency of operation |
| $r_{scat}$ | [10, 1000] $\lambda$ | Radial distance of scatterers from a transmitter |

The plot of Figure 3.4 shows the results of the simulation with parameters given in Table 3.1. As shown in Figure 3.4, the cumulative distribution function (CDF) curve of the BER for the UCA did not exceed 0.4 BER, while the CDF curve of the BER for the ULA contained values at 0.5 BER. This might seem to be a significant performance difference, but overall, the performance difference is not significant enough to draw conclusions about which array performed better.


(a) Uniform Linear Array (b) Uniform Circular Array

**Figure 3.3** Uniform Linear and Circular Arrays (ULA and UCA)

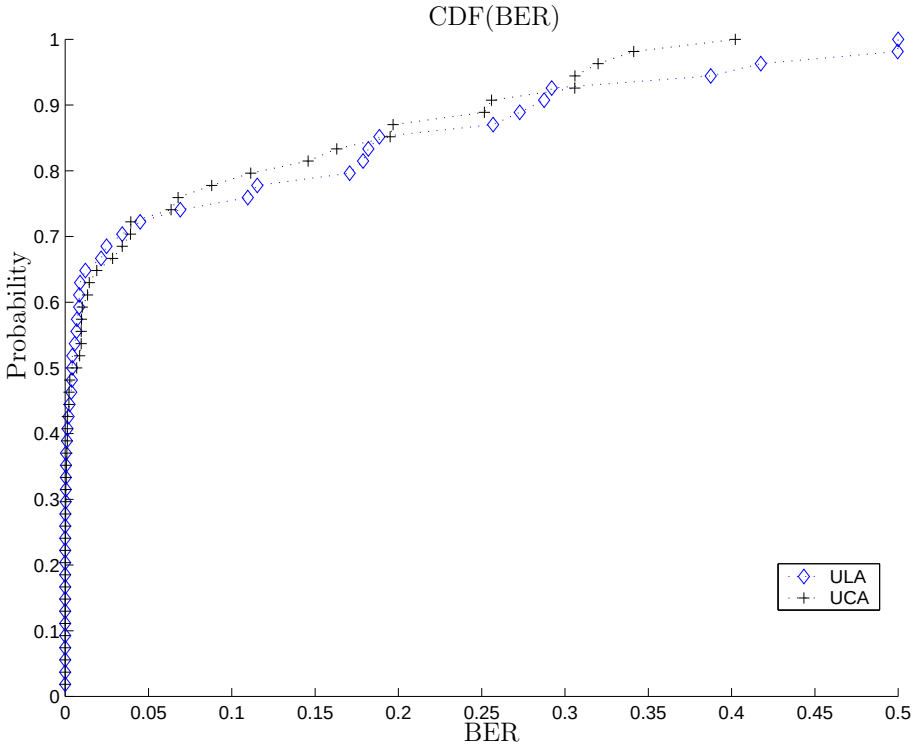


**Figure 3.4** Probability of a given bit error rate (BER) obtained by simulation set discussed in Section 3.7.1

### 3.7.2 Pattern Analysis

An example simulation is given to show the ACS pattern analysis capabilities. Throughout this section, Figure 3.5, Figure 3.6 and Table 3.2 will be referred to in describing the simulation set and results.

#### 3.7.2.1 Simulation Set

The array of choice for this simulation was the three-element triangular array of Figure 3.5. As shown in Figure 3.5, the inter-element spacing of the uniform triangular array (UTA) was equivalent to $\frac{2}{5}\lambda$. This array could be called a circular array, as all three elements are equidistant from the origin and equally spaced in azimuth.

The description of the channel is also necessary in describing the simulation set. For this particular simulation, one user was present. The user was positioned at 1 km from the receive array, in the "three-o'clock" or $0^o$ azimuth position. The channel was void of any interferers or any scattering objects. Essentially the channel was a free-space channel.

#### 3.7.2.2 Results

The simulation parameters in Section 3.7.2.1 were used as input to ACS. The results of the ensuing simulation are presented in graphical and tabulated formats (see Figure 3.6 and Table 3.2). The plot of the normalized field pattern in Figure 3.6 shows the array succesfully beamformed on the desired user. Table 3.2 provides the specifics of the pattern.

The information in Table 3.2 has been assembled after careful evaluation of a text file that was generated by ACS. This text file contains the value of the normalized field pattern for every $1^o$ in azimuth. This particular simulation showed that the triangular array produced a main beam 3 dB beamwidth = $68^o$, and a backlobe that was -18.6 dB, relative to the main beam.

The information presented in Figure 3.6 and in Table 3.2 is actual simulation data, however, it is placed here merely to provide examples of ACS capabilities. Simulation results for this thesis will be presented and discussed in context of specific simulations in Chapter 4.

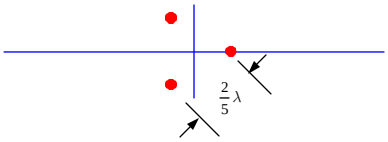


**Figure 3.5** Three-element uniform triangular array (UTA)

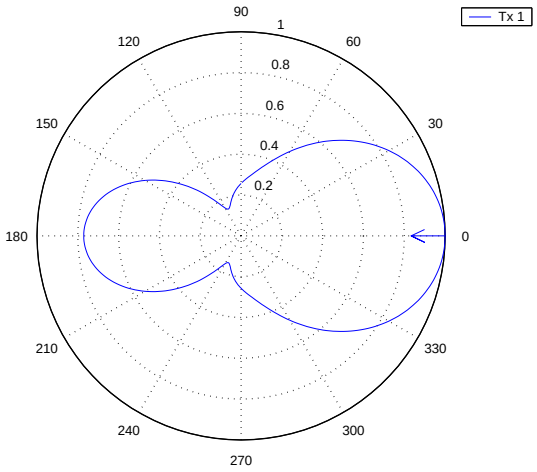


**Figure 3.6** Plot of an antenna pattern for the case of one user in the system.

**Table 3.2** An example of output data from an ACS simulation.

| Parameter | Value |
|---|---|
| User location | 1 km @ $0^0$ |
| Element Spacing | $\frac{2}{5}\lambda$ |
| $3-dB$ Beamwidth (Mainbeam) | $68^0$ |
| Major Side-Lobe Location | $@180^0$ |
| Side-Lobe Level (dB) | $-18.6$ |

## 3.8 Summary

This chapter has presented ACS and its components. In Section 3.2, the procedure of using ACS was given. Section 3.3 discussed the type of signaling that was used in the simulations. The beamformer and diversity combiner were discussed in Sections 3.4 and 3.5. The channel model was discussed in Section 3.6. The chapter concluded in Section 3.7 with a discussion of the available outputs of ACS. More simulation information will be provided in the following chapter.

# References


[1] K. P. Dietze, "Vector Multipath Propagation Simulator." VTAG Internal document, May 1999.

[2] *Digital and Analog Communication Systems*, ch. 8. Prentice Hall, 2001.

[3] B. ki Kim, *Smart Base Station Antenna Performance for Several Scenarios - an Experimental and Modeling Investigation*. PhD thesis, Virginia Polytechnic Institute & State University, Blacksburg, VA, May 2002.

[4] J. Litva and T. K.-Y. Lo, *Digital Beamforming in Wireless Communications*. Boston, London: Artech House, 1996.

# Chapter 4

# Results of Simulations that used Bit Error Rates to Quantify Relative Performance of Base Station Array Topologies

This chapter presents data for a base station array geometry[1] analysis using Bit Error Rate (BER) as the simulation criterion of relative performance. This work utilizes the Array Configuration Simulator (ACS) as discussed in Chapter 3. The motivation for the research is given in Section 4.1. Section 4.2 presents information on the array geometries for the Bit Error Rate (BER) simulations. Section 4.2 also details the use of adaptive beamforming and diversity combining by the base station array in the simulations. Section 4.3 presents information about the simulated channel. Simulation scenarios and results are discussed in Section 4.4. A summary of the chapter is provided in Section 4.5.

[1]The terms **geometry(ies)**, **topology(ies)** and **configuration(s)** are used interchangeably throughout this chapter.

## 4.1 Motivation

The base station array geometries of Figure 4.1 were simulated in an attempt to determine a 'best choice' base station array antenna configuration for a $3^{rd}$ Generation CDMA macrocell communications system. It is important to note, that 'best choice' assumes the general case, not a site-specific optimal choice. The focus of the investigation was to determine if base station array topology could be directly linked to system performance. The arrays in Figure 4.1 will be discussed in more detail in Section 4.2.

The geometries of Figure 4.1 were selected for simulation because they were presented in a published paper by J.W. Liang and A.J. Paulraj [1] to investigate cell coverage range extension. The set of array geometries provide a means to test linear vs. circular structures as well as arrays with uniformly spaced elements vs. arrays with non-uniformly spaced elements. The authors studied optimum base station array antenna topologies for coverage extension in cellular radio networks. The simulations in [1] focused on the coverage range increase that can be obtained by adding antenna elements to the array. Their simulations investigated three diversity characteristics: number of antenna elements, angle spread and array topology. The authors in [1] report that the presence of multipath in a cellular environment accounts for a breakdown of the plane wave model validity. This is due to the fact that the situation of correlated signal components arriving at different times and from various directions is much more complicated than a single plane wave from a single source. It also was a conclusion of [1] that for situations with large angle spread and a large number of antennas in the system, array topology matters little when discussing range of coverage. The paper also states that with a careful design of the base station topology, diversity can be exploited and the range coverage can be extended for a cellular network, especially when the system lacks sources of diversity (e.g. few antennas and small angle spread). As previously stated, the arrays in [1] consist of basic linear and circular geometries with modifications that introduce spatial separation to the arrays. These structures were used in the simulations in hopes they would give insight to performance of linear versus circular structures.

## 4.2 Simulated Base Station Array Configurations

The array geometries listed in Table 4.1 and shown in Figure 4.1 were implemented as base station arrays in simulations of a macrocell wireless communications system. Table 4.1 provides a categorization of the arrays. Figure 4.1 presents a graphical representation of the arrays modeled in the simulations. Table 4.1 with Figure 4.1 provides a framework to discuss the concepts of circular and linear topologies as well as the concept of uniformly spaced topologies and spatially separated topologies.

### 4.2.1 Definitions and Simulation Parameters

The simulations tested the performance of array antennas with linear and circular topologies as well as uniform and spatial topologies. Linear topologies are based on a linear geometry. Linear arrays that were simulated are shown in Figures 4.1(a) and 4.1(c). Circular topologies are based upon a circular geometry. Figures 4.1(b), 4.1(d), 4.1(e) and 4.1(f) present the circular geoemetries that were used in the simulations.

In discussing these simulations, the term 'uniform' will refer to topologies with uniform adjacent element spacing equal to one-half wavelength. Examples of uniform topologies are the Uniform Linear Array (ULA) given in Figure 4.1(a) and the Uniform Circular Array, given in Figure 4.1(b). The term 'spatial' will refer to topologies with element spacings much greater than $\frac{\lambda}{2}$, or where portions of the array are uniformly spaced, but are greatly separated (ie. $>> \frac{\lambda}{2}$) from other portions of the array. Examples of spatial topologies are given in Figures 4.1(c) - 4.1(f). All arrays in Figures 4.1(c) - 4.1(f) have some aspect of uniform spacing, but the arrays have significant separation between segments of the arrays. The large circular array (Large CA) shown in Figure 4.1(d) is comprised of uniformly spaced elements, but it is classified as a spatial topology because of the large inter-element spacing.

All arrays were simulated with elements positioned in the x-y plane (i.e. $\theta = 90^o$). The parameter $\phi$ was measured in degrees counter-clockwise from the positive x-axis of a Cartesian co-ordinate system, as shown in Figure 4.2. Each array implemented dipoles for its elements and each dipole was vertically oriented (i.e. along the z axis).

**Table 4.1** Simulated topologies

| Array Type | Array Designation | Figure |
|---|---|---|
| Uniform Linear | ULA | 4.1(a) |
| Uniform Circular | UCA | 4.1(b) |
| Linear with Spatial Separation | TwoULA | 4.1(c) |
| Circular with Spatial Separation | LargeCA | 4.1(d) |
| Circular with Spatial Separation | UCAPlusOne | 4.1(e) |
| Circular with Spatial Separation | TwoUCA | 4.1(f) |

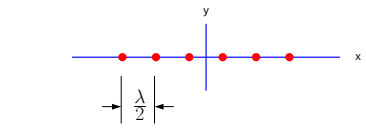


(a) Uniform Linear Array

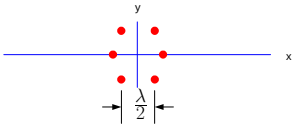


(b) Uniform Circular Array

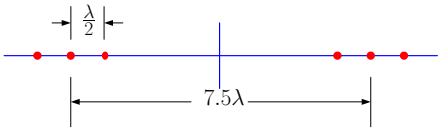


(c) Dual Uniform Linear Array

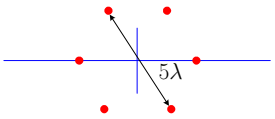


(d) Large Circular Array

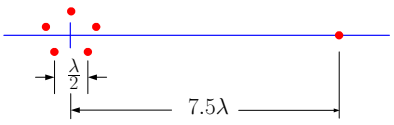


(e) Uniform Circular Array Plus One

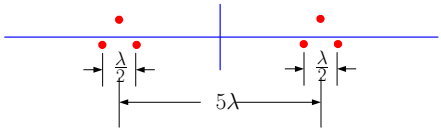


(f) Dual Uniform Circular Array

**Figure 4.1** Base station array geometries considered in the simulations.

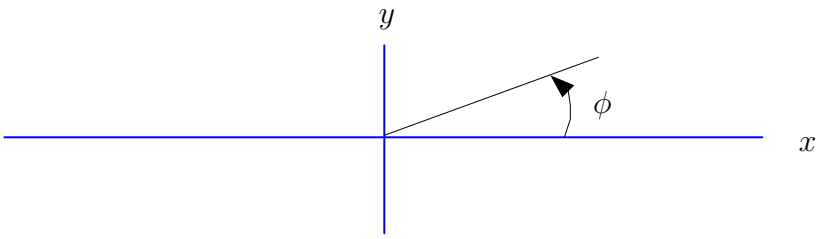


**Figure 4.2** All arrays are simulated in the $\theta = 90^o$ plane, with vertically oriented dipoles and $\phi$ measured as shown.

### 4.2.2 Use of Spatial Diversity and Adaptive Beamforming in the Simulations

The goal of implementing diversity schemes in a wireless system is to overcome signal fading. Systems with spatial diversity employ diversity combining techniques (algorithms) and widely separated antennas in an array to overcome signal fading in a channel. Selection, Equal Gain and Maximal Ratio diversity combining techniques were presented in Section 2.3. In the simulations presented in this thesis, the Maximal Ratio Combiner (MRC) technique was the diversity combining scheme of choice.

An optimal beamformer (see Sections **??** and 3.4) was implemented in the simulations conducted for this reseach. The number of antenna elements in the receive array, $M$, equalled the number of users in the system, $numTx$, for all simulations. One transmitter was chosen to be the desired transmitter and $numTx$-1 transmitters acted as interferers. Signal strength and delay spread of the multipath components were not thoroughly investigated in the simulations for this thesis. However, analysis of some of the data reveals that there was not significant delay spread of multipath components. More will be said about the multipath characteristics in Section 4.3.1

## 4.3 Simulated Channel

Using the array antennas of Figure 4.1, simulations were conducted to see if a certain topology or class of topologies outperformed others in the group. To perform a relative

comparison, system bit-error-rate (BER) was chosen as the benchmark criterion. A transmit scenario was defined by establishing transmitter locations and powers, along with scatterer locations and reflection coefficients. Each specified transmit scenario was used to evalute the relative bit error rate (BER) performance of the simulated arrays.

### 4.3.1 Transmit and Scatterer Scenarios

The reader is reminded, as discussed in Section 3.6.2.1, that all transmitted signals are independent of each other. A group of $numScat$ scatterers were specified for each specific transmitter to provide multipath signal components in the channel. Since a group of scatterers were created for each independent transmitter, the scatterers provided groups of multipath components that were correlated with specific transmitters.

The transmit and scatterer scenarios were created by establishing constraints on the location of transmitters and scatterers. The transmitters were all of equal power and were constrained to be within a radial distance, $300 \leq Txdist \leq 3000$, meters. Locations or radial distances within the interval were found using a random number generator (a MATLAB function, *rand*).

The scatterers were positioned in the x-y plane in relation to the individual transmitters, in terms of multiples of wavelengths, $\lambda$. Each group of scatterers was located within the range, $10 \leq Scatdist \leq 1000$ wavelengths from a specific transmitter. Each scatterer was assigned a reflection coefficient value of $\Gamma = 0.5$. The association of $numTx$ scatterers with each transmitter provided groups of multipath signal components that were correlated with specific transmitters. As stated previously, a significantly delayed multipath component can act as an additional effective interferer. Worst-case multipath scenarios are given below, based upon the incorporated scatter model.

The variable $Scatdist$, as given in the previous paragraph, and the frequency of interest, $freq = 2GHz$, can be used to describe the largest possible multipath delay within a system. This assumes a single bounce model is employed. The maximum value for $Scatdist$ is 1000 $\lambda$. At 2 GHz, 1000 $\lambda$ equals a distance of 150 meters. A propagating electromagnetic wave travels at the speed $c_o \cong 3e8\frac{m}{s}$. For the worst-case, a multipath component will arrive approximately 1 microsecond after any LOS component, having travelled an additional 300 meters. The symbol duration that was used for these simulations was 0.4 microsecond.

Referring again to the rule of thumb provided in [2], we see that for the multipath to be considered interference, it must arrive at least later than 0.04 microsecond. In this extreme case, the delay criterion is met for the multipath to cause inter-symbol-interference. Velocity relates distance and time, so one can see that for a delay of .04 microsecond, at a velocity of $3e8\frac{m}{s}$, this corresponds to a distance of 12 meters (80 wavelngths at 2 GHz). Essentially, any multipath path length longer than the LOS component by 12 meters or more could cause ISI.

Another necessary condition that has to be met for ISI to occur is that the delayed multipath components must be received with amplitudes that are significant relative to the LOS component. There are two aspects to the amplitude condition. First, the signal attenuation due to path loss must not be too great. The path loss calculation shows that for the scatterer model employed in the simulations, any single-bounce multipath component amplitude is within 6 dB of the received LOS component amplitude. This leads one to believe that in fact ISI is quite possible in this simulated channel. The second aspect of amplitude to be considered is that the received signal components must not add destructively at the receiver. The constructive or destructive addition of the components can be determined if the phase is known of all components at the receiver. It was the phase of the signals that was not thoroughly investigated in the simulations and therefore, it cannot be stated how much ISI was caused in the simulations.

Regardless of the lack of phase information, qualitiatively, it can be said that ISI was caused in the channel because multipath components were delayed and significant in amplitude, relative to the LOS components.

The parameters discussed here and in Section 4.3.2 are presented in Table 4.2. Please note that two of the parameters (i.e. ACS variables) have a 'TBD', or to be discussed in their value column. These parameters are not general to the simulations conducted for the study. These two parameters will be discussed specifically in Sections 4.4.1 and 4.4.2.

### 4.3.2 Notes About the Data for the Bit Error Rate Analysis

This section provides information about the BER data set and provides an analysis of the bit error rate simulation data. Each transmitted signal was comprised of a stream of 500,000 bits. The high number of transmitted bits provided a means of obtaining bit error rates in

**Table 4.2** Tabulated Parameters for the Transmit and Scatterer Scenarios

| Variable | Value | Description |
|---|---|---|
| $numScat$ | TBD | Number of scatterers per transmitter |
| $Txdist$ | [300, 3000] meters | radial distance of transmitter(s) from receive array |
| $Scatdist$ | [10, 1000] wavelengths | radial distance of scatterers from transmitter |
| $\Gamma$ | 0.5 | Reflection coefficient for scatterers |
| $numTx$ | TBD | number of transmitters in the system |
| $freq$ | 2 GHz | system operating frequency |
| $c_o$ | $3e8\frac{m}{s}$ | speed of an electromagnetic wave propagating in free space |
| $bits$ | 500,000 | number of bits transmitted by each transmitter |

conditions of relatively high $\frac{E_b}{N_o}$. Each transmitted signal used a carrier frequency, $freq =$ 2 GHz. All signals implemented BPSK modulation. Simulations were conducted using the transmit scenarios as discussed in 4.3.1 and the array geometries of Figure 4.1. The values of $\frac{E_b}{N_o}$ in the simulations were varied over the range [1,12] dB. For higher values of $\frac{E_b}{N_o}$, errors were often non-existant. In the simulation cases where one or more array provided zero bit errors for 500,000 transmitted bits, the results were discarded. These simulation results were discarded from the body of data because a BER of 0 is impossible. A BER of 0 was acheived most likely due to very good, though not perfect array performance and resolution limitations associated with the computer processing.

## 4.4 BER Analysis Results

The results of the simulations are presented in two sections. The first section, titled Preliminary Results, details the process of software validation. The second section of results, titled Final Results, gives the findings of the simulations in graphical format with comments.

### 4.4.1 Preliminary Results

Preliminary simulations were performed to see if a full study was warranted and to see if the Antenna Configuration Simulator (ACS) would provide valid results. Each of the antenna configurations of Figure 4.1 was evaluated using ACS. As stated in Chapter 3, ACS allows the user to define transmitter locations and power, scatterer locations and reflection coefficients, receive array element locations, and channel noise. For all cases, the arrays are located at the origin and oriented as previously shown in Figure 4.2.

#### 4.4.1.1 Simulation Case 1

Computations for Case 1 of the simulations were performed under the following conditions: the number of transmitters equal to the number of receive array elements (i.e. $N = 6$), the number of scatterers per transmitter, $numScat$ was also equal to 6 and the $\frac{E_b}{N_o}$ ratios of 1-4, 6,8,10,12 dB were used. The Case 1 parameters are tabulated in Table 4.3. Keep in mind that the parameters presented in Table 4.2 are also applicable to Case 1 simulations. The simulations results are expressed using the Cumulative Distribution Function (CDF) as a function of BER, as shown in Figure 4.4.

**Table 4.3** Parameter Descriptions and Values for Case 1 Simulations

| Variable | Value | Description |
|---|---|---|
| $numTx$ | 6 | Number of transmitters in the system |
| $N$ | 6 | Number of elements in the receive array |
| $numScat$ | 6 | Number of scatterers per transmitter |
| $\frac{E_b}{N_o}$ | 1-4, 6, 8, 12 dB | see Section 3.3 |
| $DesiredLoc$ | $120 \leq \phi \leq 180^o$ | Constraint on desired user in azimuth plane |

In plots of Figure 4.4, the abscissa represents the Bit Error Rate (BER) and the ordinate represents probability. The data are represented in the two graphical forms (semi-log and linear) becasue together, they provide a better description of the simulation results.

Both graphs in Figure 4.4 are constructed such that an ideal system (i.e. BER = 0), would have one vertical line along the ordinate at an abscissa value = 0; an impossibility. In fact,

the linear graph of Figure 4.4(b) is technically incorrect for showing BER = 0, as a possible value.

The semi-log plot of Figure 4.4(a) does show that there is a slight, but inconclusive difference in the relative performances of the 6-element arrays. The linear plot of Figure 4.4(b), however, reveals that there are consistent differences between the array performances. Specifically, the Cumulative Distribution Function (CDF) of the BER for the linear structure arrays (ULA and Two ULA) 'belly out'. The CDF curves for the circular structures have a much steeper rise, and therefore it can be said that lower BER values are more probable for the circular structures.

A polar plot of a transmit location scenario for the Case 1 simulations is given in Figure 4.3, seen previously in Chapter 3. Referring to Figure 4.3, notice the desired user is in the range $120^0 \leq \phi \leq 180^0$. In Figure 4.3, the base station is at the center of the plot and the radial distance is measured in meters. A single element was also simulated as a base station receive "array" in Case 1. The single element is shown to be outperformed significantly by the 6 element arrays; see Figure 4.4.

In Case 1, the transmit scenario was established such that there was one transmitter in each $60^0$ segment of the azimuthal plane. The desired user was always constrained to be within $120^0 \leq \phi \leq 180^0$. Therefore, the desired user was never permitted to be broadside to a linear array structure. Careful examination of the plot of Figure 4.4 reveals that the circular structures outperformed the linear structures. This was expected because of the location of the desired user was never broadside to the linear arrays. A linear array is best able to provide a narrow beam in the boresight (broadside) direction. A narrow beam is needed to provide gain for the desired user, while at the same time canceling interference. Since the desired was never in the region where a linear array was designed to best perform, it was expected that the circular structures would outperform the linear structures. Meeting this expectation provided some sense that ACS was a valid simulation tool. The fact that there was performance differences among the simulated arrays, did give reason to continue the study.

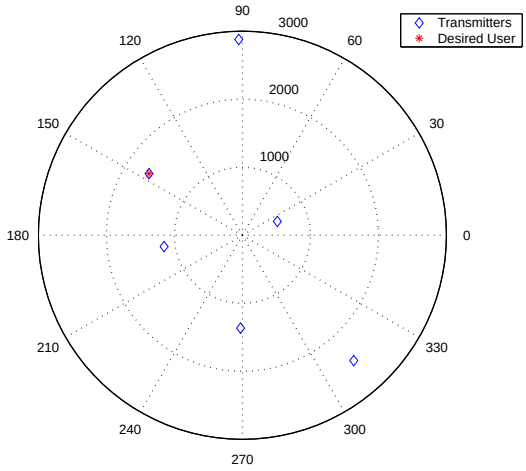


(a) A Transmit Scenario showing transmitter locations around the base station, with radial distance in meters

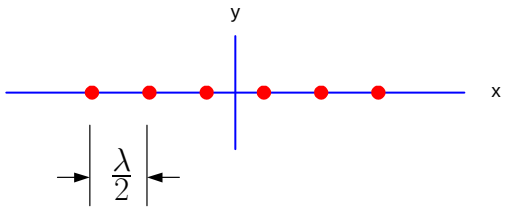


(b) Orientation of the Uniform Linear Array, located at the origin.

**Figure 4.3** A Case 1 transmit scenario and the uniform linear array depicting the orientation of the receive arrays in the simulation

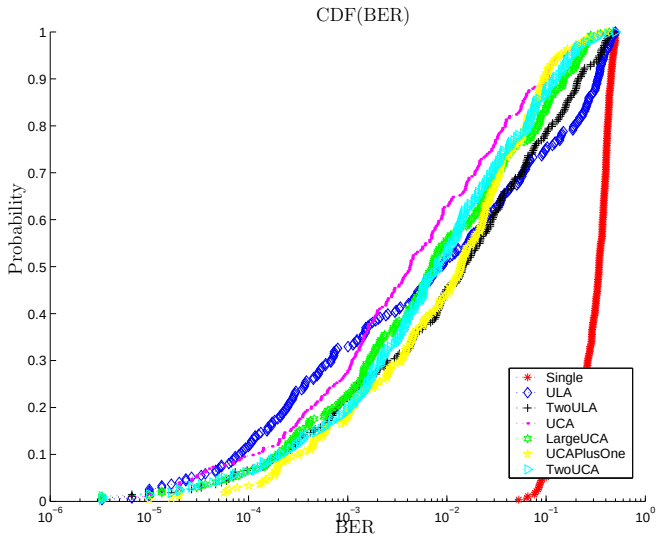


(a) Results plotted in semi-log format

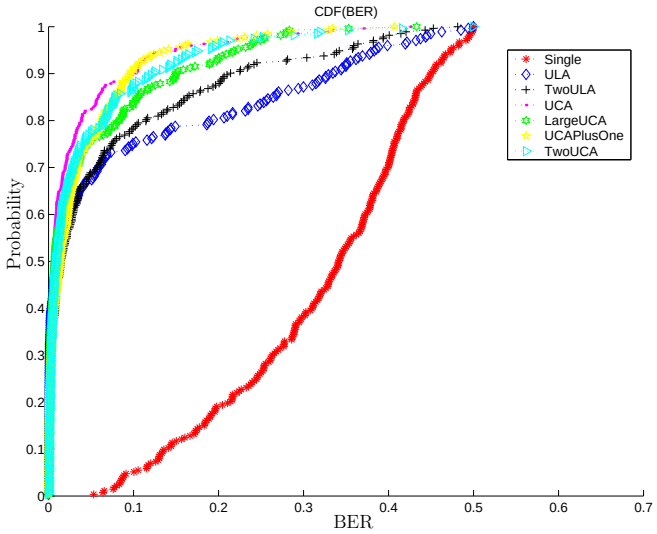


(b) Results plotted in linear format

**Figure 4.4** Probability of a given bit error rate (BER) obtained by simulation for Case 1 of Figure 4.4.1.1 for values of $\frac{E_b}{N_o} = 1, 2, 3, 4, 6, 8, 12dB$ [273 simulations].

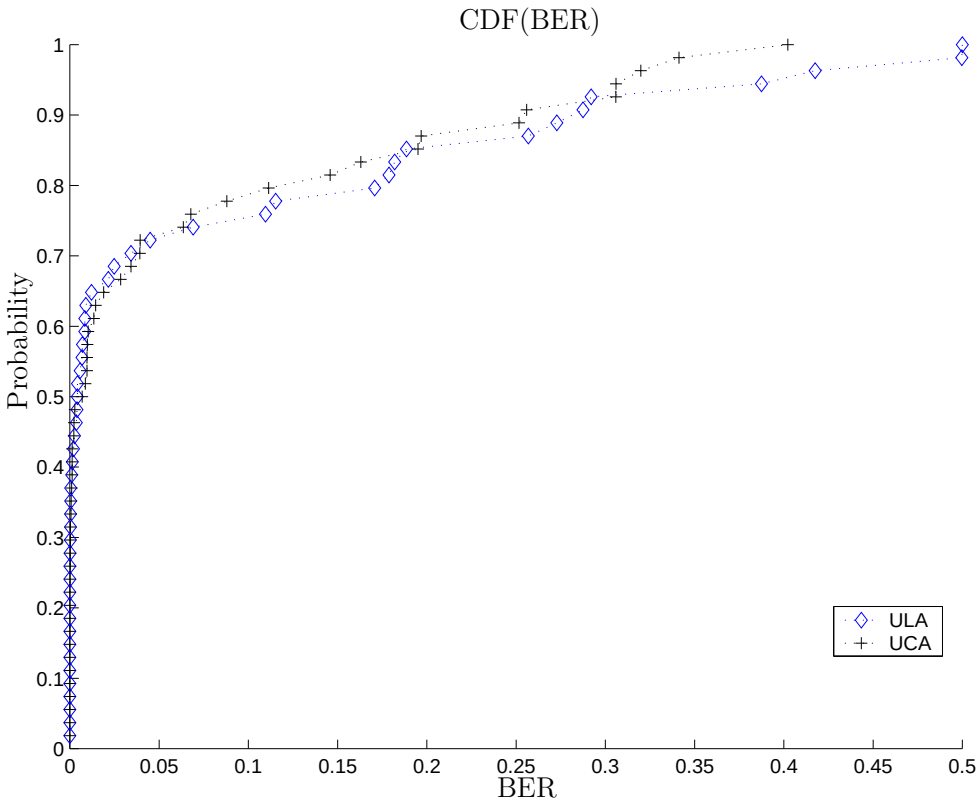


**Figure 4.5** Probability of a given bit error rate (BER) obtained by simulations for Case 2 of Section 4.4.2.1 for values of $\frac{E_b}{N_o} = 6dB$ [54 simulations].

### 4.4.2 Final Results

The simulation parameters were modified to create more freedom in the scenarios. All users in the system, including the desired user were allowed to be in the azimuthal plane for all $\phi$. This did two things. First, this change allowed the desired to be broadside to the linear structures, as well as co-linear with the linear structures. Second, the change allowed for the possibility that all users could have a uniformly distributed angle spread, or a very small localized angle spread. This provided a more realistic model.

#### 4.4.2.1 Simulation Case 2

Case 2 simulations were performed to obtain insight to array performance at a specific value for the $\frac{E_b}{N_o}$ ratio. This is in contrast to Case 1 where many values for $\frac{E_b}{N_o}$ were simulated. Also in contrast to Case 1, in the Case 2 simulations, the transmitters were allowed to be located at any angle in the azimuth plane. The radial distance constraint of $300m \leq r \leq 3000m$ was still in effect. The parameters that are specifically altered for Case 2 from those of Case 1 are given in Table 4.4. Again, the parameters of Table 4.2 are applicable to this case, Case 2.

**Table 4.4** Tabulated Parameters for Case 2 Simulations

| Variable | Value | Description |
|---|---|---|
| $\frac{E_b}{N_o}$ | 6 dB | see Section 3.3 |
| $Txdist$ | [300, 3000] meters | radial distance of transmitter(s) from receive array |
| $Desiredloc$ | any value of $\phi$ | Constraint on desired user in azimuth plane |

The results of the simulation for Case 2 are given in Figure 4.5. The graph of Figure 4.5 shows that for this environment, (i.e. $\frac{E_b}{N_o} = 6dB$), the performance was approximately equal for the linear array (Figure 4.1(a)) and the small circular array (Figure 4.1(b)). Only the results of the linear and small circular array simulations are given here because they marginally outperformed all other simulated structures. All of the structures with non-uniform spacing (Figures 4.1(c)-4.1(f)) under-performed most likely due to the fact that the non-uniform spacing caused many relatively high side lobe levels (SLL) in the array antenna pattern. The high SLL hinder interference rejection and noise cancellation in the system. It

was for this reason, that although all arrays of Figure 4.1 were simulated, only the results from the linear and the small circular arrays are shown in Figure 4.5.

It should be noted, that in the simulations run for Case 2, the performance difference between the best and worst performing arrays was very slight. It can be said that the array structures might not perform differently. A review of the plot of Figure 4.5 reveals that the CDF curves of the uniform linear array (ULA) and the uniform circular array (UCA) were not significantly different. There is not a practical improvement in system performance in implementing one array over the other.

#### 4.4.2.2 Simulation Case 3

Case 3 simulations differed from Case 2 simulations only in the value chosen for the $\frac{E_b}{N_o}$ ratio. In Case 3, the value was fixed at 1 dB. Choosing $\frac{E_b}{N_o} = 1$ dB allowed the arrays to be tested under poor conditions (i.e. a noisy environment).

The results of this set of simulations is shown in linear format in Figure 4.6. Again, the CDF curves of the linear structures 'belly out'. This seems to show that the circular structures have a higher probability of a lower Bit Error Rate (BER) than the linear structures. As in Case 2, however, careful review of Figure 4.6 shows that performance differences are not significant.

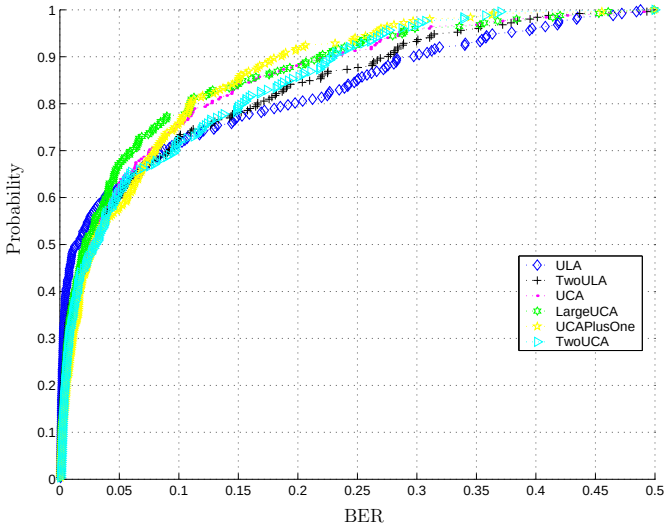


**Figure 4.6** Probability of a given bit error rate (BER) obtained by simulation for Case 3 for values of $\frac{E_b}{N_o} = 1$ dB [252 simulations].

## 4.5 Summary

The results of the simulations are presented again in Table 4.5. The purpose of Table 4.5 is to give the reader an opportunity to review simulation parameters and results of a particular simulation case in light of the other cases. It is important to note that the only significant changes among the case simulations are the signal environment ($\frac{E_b}{N_o}$) and the constraint placed upon the desired user ($\phi$) in the azimuth plane.

It is important to answer the question that was posed at the end of Section 1.1. In Section 1.1, it was asked if there was a best array topology for the general case. The answer is a qualified 'no'.

Qualifiers are presented here. The channel is a static channel; a major assumption in this thesis. The channel does contain multipath, with some of that multipath producing ISI. The channel should contain several independent users, each with an associated scatterers. The number of users should equal the number of receive array elements. Noise should be white.

Within the above constraints, it was found that generally, the arrays did not have significant performance differences. The conclusion can be drawn that topology is not important in environments similar to those simulated in Cases 2 and 3. This conclusion, that topology

**Table 4.5** Tabulated Parameters for Simulation Cases 1, 2 & 3

| Parameter | Comments | Case 1 | Case 2 | Case 3 |
|---|---|---|---|---|
| $\frac{E_b}{N_o}$ (dB) | Characterizes signal environment | 1-4, 6, 8, 12 | 6 | 1 |
| $\phi$ (degrees) | Constraint on desired user | [120,180] | [0,360] | [0,360] |
| $numTx$ | Number of transmitters in system | 6 | (for all cases) | |
| $Txdist$ (meters) | Radial distance of transmitters from receive array | [300, 3000] | (for all cases) | |
| $numScat$ | Number of scatterers per transmitter | 6 | (for all cases) | |
| $\Gamma$ | Scatterer reflection coefficient | 0.5 | (for all cases) | |

matters little, supports the findings in [1], that topology is not important in arrays with a large number of elements.

This chapter provided the background and results of the simulations conducted using BER as a means of comparing relative array performance. The chapter started with providing the motivation for the simulations in Section 4.1. A few defintions and parameters particular to the simulations were presented in Section 4.2. The specifics of the diversity combining and array beamforming implemented in the software was also in Section 4.2. The channel model was presented in Section4.3 and the chapter concluded with a presentation of the simulation results in Section 4.4. The reader is reminded that background for these simulations was presented in Chapters 2 and 3.

# References

[1] J.-W. Liang and A. J. Paulraj, "On optimizing base station antenna array topology for coverage extension in cellular radio networks," in *1995 IEEE 45th Vehicular Technology Conference*, vol. 2, pp. 866–870, 1995.

[2] K. P. Dietze, "Analysis of a two branch maximal ratio and selection diversity system with unequal branch powers and correlated inputs for a rayleigh fading channel," Master's thesis, Virginia Polytechnic Institute & State University, Blacksburg, VA, March 2001.

# Chapter 5

# Conclusion

This thesis presented a simulation analysis of array geometries for wireless communications. Chapter 2 of the the thesis reviewed topics of array theory, beamforming, diversity combining, and channel modeling. Chapter 3 combined many of the basic theory elements in the discussion of a simulation tool, the Antenna Configuration Simulator (ACS), used in the simulation work of the thesis. Chapter 4 provided results of various simulations performed using ACS.

Specifically, the thesis presented data on array operation in wideband communication systems. In Chapter 4 it was shown that uniform structures outperformed spatial structures and circular structures outperformed linear structures. This is due largely to the fact that the simulations presented channels with interference. Even though a diversity combining scheme (MRC) was used in the ACS algorithm, the performance of the array relied heavily upon the beamformer for interference rejection. Though diversity does provide a gain in received signal, relative to the faded signal, realized diversity gain only is achieved once all interference has been mitigated. This thesis work showed that in an environment with a lot of interferers, the rejection of those interferers by an array is most important.

# Vita

Derek A. Wells was born September 27, 1973. Most of his childhood was spent in Lindley, NY. Upon graduating from Corning-Painted Post West High School in 1992, he attended Liberty University in Lynchburg, VA, where he graduated in 1996 with a Biblical Studies Degree and met his future wife, Staci. He married in June of 1998, while pursuing his BSEE degree in the state of South Carolina. He graduated from the University of South Carolina in May 2000 and subsequently started work for the Virginia Tech Antenna Group (VTAG)in Blacksburg, VA. Mr. Wells conducted simulation work for VTAG over the next two years, completing his service as a Graduate Research Assistant (GRA) in May 2002. In January 2003 he completed the MSEE program at Virginia Tech.